Hydrol. Earth Syst. Sci. Discuss., https://doi.org/10.5194/hess-2019-152
Manuscript under review for journal Hydrol. Earth Syst. Sci.
Discussion started: 23 April 2019

Hydrology and Earth System Sciences
Open Access
Discussions

High-resolution hydrometeorological modelling of the June 2013 flood in southern Alberta, Canada

Vincent Vionnet[1], Vincent Fortin[2], Etienne Gaborit[3], Guy Roy[2], Maria Abrahamowicz[2], Nicolas Gasset[3], John W. Pomeroy[1]

[1] Centre for Hydrology, University of Saskatchewan, Saskatoon, SK, Canada
[2] Environmental Numerical Research Prediction, Environment and Climate Change Canada, Dorval, QC, Canada
[3] Environmental Numerical Prediction Development, Meteorological Service of Canada, Environment and Climate Change Canada, Dorval, QC, Canada

Correspondence to: Vincent Vionnet (vincent.vionnet@usask.ca)

Abstract. From June 19 to June 22, 2013, intense rainfall and concurrent snowmelt led to devastating floods in the Canadian Rockies, foothills and downstream areas of southern Alberta and southeastern British Columbia. The complexity of the topography in the mountain headwaters, presence of snow at high elevations and other factors challenged hydrological forecasting of this extreme event. In this study, the ability of the Global Environmental Multi-scale hydrological modelling platform (GEM-Hydro), running at a 1-km grid spacing, to simulate hydrometeorological conditions in several Alberta rivers during this event is assessed. Four quantitative precipitation estimation (QPE) products were generated using the Canadian Precipitation Analysis (CaPA) system by varying (i) station density and (ii) horizontal resolutions (10, 2.5 and 1 km) of the GEM precipitation background. CaPA at 2.5 and 1 km including all available stations in the headwaters provided the most accurate estimation of intensity and total amount of precipitation during the flooding event. Using these products to drive GEM-Hydro, it is shown that QPE accuracy dominates the ability to predict flood volumes. Initial snow conditions also represent a large additional source of uncertainty. Default GEM-Hydro simulations starting with almost no snowpack at high-elevations led to a systematic underestimation of flood volume and peak flow. Gridded estimates of snow water equivalent from the Snow Data Assimilation System (SNODAS) were also considered. They led to contrasting abilities to simulate flood discharge volumes and a consistent overestimation in the headwater catchments, illustrating the strong need for a reference snow product in the mountains of Western Canada. Finally, GEM-Hydro did not predict peak flow timing and hydrograph shape well. Model sensitivity tests show that it could be improved by adjusting the Manning coefficients, suggesting the need to revisit the routing parameters. There may be a need to include water management effects on flood hydrographs as well. These results will guide the development of GEM-Hydro as a hydrological forecasting system in Western Canada.

Hydrol. Earth Syst. Sci. Discuss., https://doi.org/10.5194/hess-2019-152
Manuscript under review for journal Hydrol. Earth Syst. Sci.
Discussion started: 23 April 2019

1 Introduction

From June 19 to 22, 2013, heavy rainfall and snowfall (at high elevations) with local amounts exceeding 300 mm fell over a broad region of the Canadian Rocky Mountains of southeastern British Columbia and southwestern Alberta, and the foothills and adjacent plains of southern Alberta, Canada (Milrad et al., 2015; Liu et al., 2016; Kochtubajda et al., 2016; Pomeroy et al., 2016). This heavy precipitation resulted from moisture convergence from the Pacific and from the Canadian Prairies and US Great Plains through evapotranspiration (Milrad et al., 2015; Li et al., 2017). At high elevations, rain and then snow fell on a deeper than normal, late-lying snowpack leading to rain-on-snowmelt which enhanced runoff generation (Fang and Pomeroy 2016; Pomeroy et al., 2016a). This heavy rainfall combined with a rapidly melting alpine snowpack triggered severe flooding in the Oldman, Bow and Red Deer river basins of southern Alberta and the Elk River of southern British Columbia and impacted many communities, including Calgary, the largest city in Alberta (Pomeroy et al., 2016). The floods led to the evacuation of 100,000 people and caused five fatalities and over $6 billion of damage to infrastructure such as roads, railways, bridges, parks and homes (Pomeroy et al., 2016).

This extreme weather event has been investigated in details in the last few years from the perspectives of atmospheric and climate modelling. Li et al. (2017) showed that the Weather Research and Forecast (WRF) atmospheric model at convection-permitting resolution (3-km) demonstrated reasonable skill in simulating the spatial and temporal evolution of precipitation patterns before and during the flood. They investigated with the model the dynamical features that led to the generation of heavy rainfall. Milrad et al. (2017) carried out sensitivity experiments with the WRF model at the same resolution as Li et al. (2017) to determine the impacts of local topography on the extreme rainfall event. Teufel et al. (2017) presented complementary results using the Canadian Regional Climate Model at lower resolution (0.11°) than WRF. In particular, they showed that wet antecedent soil moisture conditions in the Canadian Prairies and US Great Plains impacted precipitation patterns, intensities and amounts through enhanced evapotranspiration in these upwind regions.

Despite its severe hydrological consequences, this extreme weather event has received little attention from a hydrological modelling point of view. Teufel et al. (2017) discussed the impact of initial snow and soil conditions on the amplitude and timing of streamflows. However, their study only used daily discharges from one hydrometric station located in Calgary along the Bow River for model evaluation, and this station was heavily impacted by reservoir regulation making it unsuited for this purpose. Li et al. (2017) and Milrad et al. (2017) did not use their high-resolution WRF simulations to generate hydrological simulations of the flood. At the local scale, Fang and Pomeroy (2016) studied in detail the impact of antecedent soil moisture and snowpack conditions on runoff generation during the flood for a small (9.4 km^2) and well-instrumented mountain research basin. Pomeroy et al. (2016a) used the data from the same basin to better understand and simulate the complex rain-on-snowmelt runoff generation during the event. They showed that successful modelling of the event at small scales required detailed consideration of precipitation phase, rain-on-snow processes, slope/aspect impact on snowpack energetics, forest canopy-hydrological process interactions, antecedent soil moisture, sub-surface storage and routing of runoff water through both sub-surface and overland flow pathways. However, the modelling studies mentioned here did not

evaluate the potential and limitations of large-scale hydrological models to simulate the dynamics of the flood at hourly time scales over large river basins. Furthermore, within the context of the development of a national hydrological forecasting system for Canada (GWF project, 2018), there is a need to better assess the ability of the hydrological systems currently used in Canada to simulate such extreme events.

In the recent years, Environment and Climate Change Canada (ECCC) has developed the Global Environmental Multi-scale hydrological modelling platform (GEM-Hydro, Gaborit et al. 2017). GEM-Hydro combines the GEM-Surf surface prediction system (Bernier et al., 2011) including the SVS (Soil, Vegetation and Snow) land surface scheme (Alavi et al., 2016; Husain et al., 2016) and the WATROUTE routing scheme (Kouwen, 2010). GEM-Hydro is designed "to perform reliable streamflow simulations with a distributed model over large and partly ungauged basins" (Gaborit et al., 2017). The model follows the same approach as the Weather Research and Forecasting Model hydrological modelling system (WRF-Hydro, Gochis et al., 2015) and applies a land surface scheme to calculate hydrological processes, with runoff converted to streamflow using hydrological routing. Such an approach was initially developed for Numerical Weather Prediction (NWP) despite limitations in the representation of spatial variability of hydrological processes in such schemes (Clark et al., 2015). WRF-Hydro serves as the core model for the United States National Water Model (Maidment, 2017). GEM-Hydro has been evaluated in details in the Great Lakes region (Gaborit et al., 2017) and is a component of the Water Cycle Prediction System which provides daily operational forecasts of streamflow and lakes level in this region (Durnford et al., 2018). However, the skill of GEM-Hydro during extreme rainfall and snow melting events in mountainous terrain is still largely unknown.

The primary objective of this study is to evaluate the ability of GEM-Hydro to reproduce the observed hydrology in hindcast mode for the June 2013 flood in southern Alberta. Another main objective is to assess the sensitivity of hydrological simulations to the main factors controlling flood dynamics, such as precipitation forcing accuracy, initial snowpack conditions and river routing parameters. For this purpose, a specific configuration of the Canadian NWP model GEM (Côté et al., 1998; Girard et al., 2014) was deployed over the region to produce atmospheric forcing at resolutions ranging from 1 to 10 km to drive GEM-Hydro. In particular, the precipitation simulated by GEM was combined with precipitation gauge measurements from different observation networks using the Canadian Precipitation Analysis (CaPA) system (Mahfouf et al., 2007; Lespinas et al., 2015; Fortin et al., 2018) to generate several quantitative precipitation estimation (QPE) products for the flood. These products were used to assess how QPE accuracy influences the uncertainty in simulating streamflow from the mountain headwaters downriver to cities that were impacted by the flood such as Calgary and High River. The role of initial snowpack conditions at high elevations prior to the flood and uncertainties in river routing parameters were also considered.

The paper is organized as follows. Section 2.1 presents the study area and the different datasets used in our study. It also describes the GEM-Hydro modelling platform and the configurations of the different experiments carried out with this model in our study. Section 3 evaluates the different hydrological inputs used in this study (initial snowpack conditions, QPE

products) and the resulting hydrological simulations. Section 4 contains a discussion of the main results of this study. Finally, concluding remarks are presented in Section 5.

2. Data and Methods

2.1 Study area and data

The study area covers the three main river basins in southern Alberta that were strongly impacted by the June 2013 flood: the Red Deer, Bow and Oldman river basins (Fig. 1). These rivers drain the Rocky Mountains and their foothills, flowing eastward towards the Canadian Prairies and eventually joining to form the South Saskatchewan River. The black box in Fig. 1 highlights the location of the Elbow and Highwood rivers - both spilled over their banks during the flood, affecting the cities of Calgary and High River.

Precipitation data were obtained from four different networks (Fig. 1). Automatic synoptic stations (SYNOP network) maintained by Environment and Climate Change Canada and other organizations such as Alberta Agriculture and Forestry provide a good coverage over the prairies and the forested foothills but only a sparse coverage of the Canadian Rockies, particularly in Banff National Park where the stations are mainly located in the valleys (see for example the upper Bow river basin, Fig. 1). Therefore, to fill in data gaps, precipitation data were taken from Alberta Environment and Parks because of their good coverage of the higher elevations of the Canadian Rockies headwaters. Data from high elevation mountain stations of the Canadian Rockies Hydrological Observatory (CRHO, University of Saskatchewan, https://www.usask.ca/hydrology/CRHO.php) were also used in the upper Bow River Basin. Finally, stations from the American Cooperative Observer Network (COOP) reporting 6-h precipitation amounts were included. Theses stations are mainly located in the US and on the western side of the study area and were referred as stations from the SHEF network (Standard Hydrometeorological Exchange Format) in Lespinas et al. (2015). They were not included in the 6-h operational precipitation analysis at the time of the flood.

Information on snow conditions before the flooding event and during the winter of 2012/2013 were obtained from 11 automatic snow pillows from Alberta Environment and Parks located in southern Alberta. These stations measure hourly snow water equivalent (SWE). Additionally, outputs from the SNOw Data Assimilation System (SNODAS) from the US National Operational Hydrologic Remote Sensing Center (NOHRSC) were included in this study. SNODAS estimates various snow properties (including SWE and snow depth) by merging satellite, airborne, and ground-based snow data with a numerical simulation of snowcover (Barrett, 2003). SNODAS data are available at 1-km spatial resolution and 24-hour temporal resolution and cover continental US as well as part of Canada (up to 54° N). In southern Alberta, the snow pillows from Alberta Environment and Parks are included in SNODAS since they provide relevant information for mountain snow conditions, including those affecting the Columbia River flowing from Canada to the US. The ECCC snow analysis (Brasnett, 1999) was not considered in our study since its spatial resolution (10 km) is too coarse to accurately represent

snow conditions in the complex topography of the Canadian Rockies. Moreover, the ECCC snow analysis only contains information on snow depth and therefore lacks the crucial information that SWE is for hydrology.

Hourly streamflow time series were obtained from the Water Survey of Canada for stations located in the Jumpingpound Creek, Elbow River and Highwood River basins (Fig. 2). These rivers were selected for the evaluation of GEM-Hydro simulations since they were strongly impacted by the flood and are only slightly affected by regulation. Two stations were destroyed during the flooding event and removed from the study. Overall, 10 stations were kept for the evaluation of hydrological simulations (Fig. 2).

2.2 The GEM-Hydro modelling platform

GEM-Hydro is a distributed runoff-modelling platform developed at ECCC for hydrological modelling across Canada (Gaborit et al., 2017). It is composed of two components: (i) the GEM-Surf surface prediction system (Bernier et al. 2011) and (ii) the WATROUTE routing scheme (Kouwen, 2010). GEM-Hydro has been extensively evaluated over the Great Lakes (Gaborit et al., 2017) and is a component of the Water Cycle Prediction System running operationally at ECCC over the Great Lakes and St. Lawrence River watershed (Durnford et al., 2018).

GEM-Surf simulates the evolution of six types of surfaces: land, glacier, inland water, sea, ice (over sea or lake) and urban areas. Over land, it uses the SVS (Soil, Vegetation and Snow) land surface scheme (Alavi et al., 2016; Husain et al., 2016). SVS relies on a multiple energy budget approach to solve the energy and mass balance at the earth surface. The land tile is divided into three main covers: bare ground, low vegetation and high vegetation. Then, SVS solves independent energy budgets using a force restore approach for bare ground, vegetation, snow covering bare ground and low vegetation, and snow below high vegetation (Husain et al., 2016). SVS uses a single-layer energy balance scheme to simulate the snowpack evolution. Hydrological processes are represented in SVS using a multi-layer scheme and assuming Darcian flow between the soil layers (Alavi et al., 2016). SVS simulates surface runoff using lateral flow for sloping surfaces (Soulis et al., 2011) and base flow at the bottom layer. WATROUTE routes surface runoff, lateral flow and base flow produced by SVS to the basin outlet. In WATROUTE, runoff and lateral flow directly feed the streams while base flow is provided to a lower zone storage (LZS) compartment, representing surficial aquifers, which releases water to the streams.

2.3 Model configuration and experiments

In this study, GEM-Hydro was used in a stand-alone (offline) mode to produce a hindcast of the hydrology of the June 2013 flood. The model was driven by a new set of atmospheric data combining short-term numerical weather forecast and precipitation analysis. These atmospheric forcings were produced at different resolutions to assess the sensitivity of GEM-Hydro to the resolution of forcing data. The impact of initial snow conditions on streamflow simulation was also assessed. In the following, the main features of the new atmospheric forcing data are detailed, as well as the different experiments carried out with GEM-Hydro.

Hydrol. Earth Syst. Sci. Discuss., https://doi.org/10.5194/hess-2019-152
Manuscript under review for journal Hydrol. Earth Syst. Sci.
Discussion started: 23 April 2019

2.3.1 Atmospheric simulations

The latest operational version of the GEM NWP model used at ECCC (Côté et al., 1998; Girard et al., 2014; Caron et al., 2015; Milbrandt et al., 2016) was used to recreate the atmospheric conditions during the flooding event. GEM was configured with three one-way nested domains with 10, 2.5 and 1-km grid spacing centred over the study area in southern Alberta. This nested approach has been applied in previous studies at ECCC (e.g. Vionnet et al., 2015; Leroyer et al., 2018). Two domains at the kilometre scale (2.5 and 1 km) were used since the previous studies of Li et al. (2017) and Milrad et al. (2017) showed that models at convection-permitting resolution performed best for this event. Details of the simulation domains are listed in Table 1. Figure 3 shows the extents of the 2.5 and 1-km grids over western Canada. Table 1 also details the physical parameterizations used in GEM at different resolutions. The model at 10-km grid spacing has the same settings as the operational version of the Regional Deterministic Prediction System (RDPS, Caron et al. 2015) used at ECCC. The 2.5 and 1-km grids used the latest configuration of the High Resolution Deterministic Prediction System (HRDPS, Milbrandt et al., 2016) which includes the P3 microphysical scheme (Predicted Particle Properties, Morrison and Milbrandt, 2015). Land surface characteristics were specified at each grid cell of each domain using different geophysical datasets described in Table 2.

GEM produced 12-h meteorological forecasts, launched 4 times per day (at 00, 06, 12 and 18 UTC) from 18 June 2013 00 UTC to 22 June 2013 12 UTC. Initial and lateral boundary conditions for the 10-km GEM model were taken every hour from the analysis and forecasts of the operational RDPS which covers most of North America. The 2.5-km (1-km) GEM model used lateral boundary conditions obtained from the 10-km (2.5-km) GEM model every 12 minutes. Model variables were stored at an hourly frequency. GEM forecasts at different resolutions are available on the Federated Research Data Repository (Vionnet et al., 2019).

2.3.2 Precipitation analysis

To test their influence on the hydrology of the June 2013 flooding event, as simulated by GEM-Hydro, new QPE products were generated. They relied upon the Canadian Precipitation Analysis (CaPA) system (Mahfouf et al., 2007; Lespinas et al., 2015; Fortin et al., 2018). CaPA combines precipitation observations with a background field obtained from a short-term meteorological forecast using optimal interpolation to produce a QPE on a regular grid. Precipitation observations consisted of rain gauges and radar QPEs (Fortin et al., 2015). The current operational version of CaPA at ECCC produces 24-h and 6-h QPE at 10-km resolution over a domain covering most of North America and at 2.5-km resolution over a domain covering most of Canada (Fortin et al., 2018).

Four precipitation datasets (6-h accumulation) were produced using CaPA for the June 2013 Flood (from 18 June 2013 12 UTC to 22 June 2013 12 UTC) with the aim of evaluating the impact of (i) assimilated station density (in particular in the Canadian Rockies, and (ii) precipitation background resolution on the QPE products and the hydrological response simulated by GEM-Hydro. The resolution of the various precipitation forcing data was that of the GEM atmospheric simulations

described in Sect. 2.3.1. The forecast used to generate precipitation forcing data had a lead time between 6 and 12 hours to avoid spin-up errors. Indeed, the precipitation amounts are currently underestimated during the first few hours of the forecast. The first CaPA experiment (*CaPA 10 km Def*) combined the observations from the SYNOP stations (Sect. 2.1) with a precipitation background from GEM at 10-km grid spacing. This CaPA configuration is similar to the one used operationally by ECCC at the time of the flooding event. Additional stations from the ABE, CHRO and COOP networks (Sect. 2.1) were then considered in the precipitation analysis in combination with precipitation background at 10, 2.5 and 1 km. These additional stations substantially increase the density of stations in the Rockies and their foothills (Fig. 1). Radar data were not included in the different QPE products since they tend to underestimate precipitation amounts in this mountainous region for this event (Kochtubajda et al., 2016). Table 3 summarizes the main characteristics of each CaPA experiment. The data from each CaPA experiment are available on the Federated Research Data Repository (Vionnet et al., 2019).

2.3.3 Surface and hydrological modelling

GEM-Hydro was used to simulate the evolution of the surface and hydrological conditions during and after the flooding event (from 18 June 2013 12 UTC to 26 June 2013 12 UTC). GEM-Hydro simulations combine successive integration of GEM-Surf (including SVS) and WATROUTE. In our study, GEM-Surf ran on the same grid and used the same geophysical fields as GEM 1 km (Tables 1 and 2). Seven layers down to 1.4 m depth were used to represent the vertical layering of soil, following Gaborit et al. (2017). The routing with WATROUTE was implemented over a 1-km grid covering the Red Deer, Bow and Oldman river basins (Fig. 1). Flow directions were derived from the HydroSHEDs database (Lehner et al., 2008). The default (uncalibrated) version of GEM-Hydro was used in the study. Parameters in SVS were the same as in the version of SVS used for NWP (Alavi et al., 2016; Husain et al., 2016). Parameters in WATROUTE were derived using the standard procedures implemented in the operational hydrological system of ECCC (Durnford et al., 2018). In particular, two Manning's roughness parameters are used for flood plain flow, n_f, and channel flow, n_c, based on values derived from the literature (Chow, 1959). n_f varies spatially with vegetation type (0.035 for low vegetation and 0.075 for high vegetation) and seasonally to represent temporal changes in vegetation. For channel flow, the value of n_c is affected by the roughness of the channel surface on the bottom and sides as well as the roughness of the underside of the ice cover overlying the river when ice is present. It varies with drainage area between 0.03 and 0.05 to represent the overall decrease of Manning coefficient from the headwaters to the river mouth (Decharme et al. 2010). These variations are effective at large scale and over our region of interest, n_c is almost constant, equals to 0.044. Calibrating GEM-Hydro is a challenging task due to model computation time (Gaborit et al., 2017). The main purpose of GEM-Hydro as used by ECCC is to produce hydrological simulations over large river basins including ungauged basins. Therefore, the model has to be able to produce reasonable simulation accuracy with default parameters, because it is difficult to obtain maximized local performances when calibrating a hydrological model over large area. Calibrating it locally on each gauge from upstream to downstream is not feasible in

practice due to model computation time, and would violate parameter consistency in space as well as lack robustness in time (Gaborit et al., 2017). For these reasons, GEM-Hydro was not calibrated in this study.

Eight simulations of the flood were carried out with GEM-Hydro. They differ in terms of resolution of the atmospheric driving data, precipitation forcing and initial conditions. Table 4 describes their main characteristics. The atmospheric forcings required for GEM-Surf include shortwave and longwave irradiation at the surface, surface pressure, air temperature, specific humidity, precipitation, and wind. Continuous atmospheric forcings from 18 to 22 June were obtained from successive GEM forecasts at different resolutions (Table 1). For the period of 22nd to 26th June, only operational forecasts of the RDPS at 10-km resolution were used as forcings. In all instances, forecast hours 6 to 11 were used to avoid spin-up errors. For the forecasts at 10 and 2.5 km, surface pressure, air temperature, humidity, and precipitation phase were downscaled to correct for elevation differences between the grid of the forecasts and the 1-km grid used by GEM-Surf as in Bernier et al. (2011). The different precipitation datasets produced with CaPA were used as precipitation forcing data (Table 3). Six-hourly precipitation outputs from CaPA were then disaggregated into hourly accumulations in accordance with the temporal precipitation structure of the GEM forecast.

Initial conditions for the surface variables on 18 June 2013 12 UTC were taken from two different 1-km GEM-Surf experiments running. Both experiments were initialized on June 1st, 2012 using RDPS 10-km surface fields interpolated to the 1-km grid and then integrated for more than one year until 18 June 2013 12 UTC to allow a sufficient spin-up of surface variables, especially soil moisture. The hourly meteorological forcings for this one-year spin-up period were taken from successive RDPS forecasts at 10-km resolution issued 4 times per day (00, 06, 12 and 18 UTC). Similarly to all other experiments, 6-11 forecast hours were used. The meteorological forcing was then downscaled to the 1-km GEM-Surf grid using the method described in Bernier et al. (2011). Following Carrera et al. (2010), precipitation was taken from the RDPS from 1 November 2012 to 30 April 2013 and from the operational version of CaPA at 10 km for the rest of the period. CaPA underestimates solid precipitation amounts (Schirmer and Jamieson, 2015), since the precipitation gauges used in CaPA are prone to wind-induced undercatch of winter precipitation (Fortin et al., 2018).

In the first experiment, *OPL*, simulated snow conditions evolved in response to the atmospheric forcing without constraint from observations. Using a similar setup, Carrera et al. (2010) and Separovic et al. (2014) have shown that GEM-Surf tends to underestimate snow water equivalent on the ground (SWE) since the 10-km forcing from RDPS does not resolve local topographic snowfall enhancement. For this reason, a second experiment, *SND*, used estimated SNODAS SWE to correct GEM-Surf modelled SWE over the region (Sect. 2.1). The correction was carried out on May 1st 2013, close to peak SWE to adjust for over-winter bias in accumulated precipitation. On that date, simulated snow depth in GEM-Surf was used to estimate SWE using simulated snow density, and this SWE was adjusted to match SNODAS SWE. After insertion on May 1st, the *SND* simulation kept running until 18 June 2013 12 UTC using the same atmospheric forcing as simulation *OPL*. The *OPL* and *SND* simulations provide two estimates of initial snow and soil conditions at the beginning of the flooding event (18 June 2013)

Hydrol. Earth Syst. Sci. Discuss., https://doi.org/10.5194/hess-2019-152
Manuscript under review for journal Hydrol. Earth Syst. Sci.
Discussion started: 23 April 2019

3.Results

3.1 Initial snow conditions

Figure 4a and 4b compare simulated initial SWE on May 1st 2013 from the two experiments. This is when SNODAS SWE was inserted into the *SND* simulation (see Sect. 2.3.3). Both simulations present similar large scale snowcover patterns with snow absence in the prairies extending north-eastward of the study area and in the low elevation Columbia River Valley of British Columbia and its tributaries. However, the simulations differ substantially in their estimation of SWE. The *OPL* simulation shows less SWE than does *SND* in the mountain headwaters of the Bow, Oldman and Red Deer river basins. A comparison of *OPL* simulations with SWE observations from ABE's snow pillows (Fig. 4c) reveals a general underestimation of SWE (except in the upper Red Deer River Basin). *SND* presents a better agreement with snow pillow SWE observations (Fig. 4d), except for the upper Elbow and Highwood river basins. Such agreement was expected since SWE observed by ABE snow pillows is included in the SNODAS analysis. The insertion of SNODAS SWE in the *SND* simulation strongly modified the high mountain snowpack conditions prior to the flooding event as shown on Fig. 4e and 4f. Very little snow remained in the *OPL* simulation, which is inconsistent with the presence of high mountain snow reported prior to the flood (Liu et al., 2016; Pomeroy et al., 2016a,b). On the other hand, the *SND* simulation predicted the persistence of snowpacks at high elevations prior to the event, mainly in the Upper Bow River Basin (detailed topographical heights are given in Fig. 1) which is consistent with observations in the region.

3.2 Quantitative precipitation estimation

Figure 5a shows the cumulative precipitation over the region during the 3-day flooding event obtained with *CaPA 10 km Def*. Regions with cumulative precipitation depths exceeding 200 mm are found on the foothills of the Rockies, mainly in the Bow River Basin. This precipitation pattern is similar to the one obtained with the operational version of CaPA at the time of the flood (not shown). Indeed, both precipitation analyses have the same horizontal resolution and include the same stations from the SYNOP network (Sect. 2.3.2). The operational CaPA analysis was used in previous studies to better understand the flood dynamics (Milrad et al., 2015) and to evaluate atmospheric models (Liu et al., 2016; Milrad et al., 2017; Teufel et al., 2017). Stations from the CRHO, COOP and ABE networks were not included in this reference precipitation analysis and were used on Fig. 5b to provide an independent evaluation of *CaPA 10 km Def* over the Rockies and their foothills. Cumulative precipitation was underestimated at most of the stations, in particular in the upper Elbow and Highwood river basins.

The introduction of CRHO, COOP and ABE stations in the precipitation analysis (*CaPA 10 km New*) modified the pattern of cumulative precipitation during the flood (Fig. 6a and d), even as the precipitation background at 10-km grid spacing remained the same between the two simulations (Table 3). In agreement with Fig. 5b, the new stations led to an increase in the estimation of cumulative precipitation in the upper Elbow and Highwood river basins where local maxima were estimated to have exceeded 250 mm. Larger cumulative precipitation was also found in the Upper Bow River Basin and

locally in the Oldman River Basin. The foothills of in the Red Deer River Basin are the only place in southern Alberta where the new analysis led to a decrease in cumulative precipitation. The resolution of the precipitation background also affects the precipitation analysis as shown in Fig. 6. Additional details associated with the influence of the topography on the precipitation background are seen at 2.5 km (Fig. 6c) and at 1 km (Fig. 6e) in areas of complex terrain, especially in the Bow River Basin.

Figure 7 shows an evaluation of the different QPE products against CRHO, COOP and ABE station observations. For *CaPA 10 km Def* , which does not assimilate these 3 networks, this is an independent evaluation. For the other datasets, a "leave-one-out" cross validation method was used, where stations are removed one by one and an analysis value is estimated at their location using stations in the vicinity, following Lespinas et al. (2015). This analysis value was then compared to that observed. Figure 7a shows that *CaPA 10 km Def* captured the general tendency of observed cumulative precipitation but missed the highest precipitation amounts, in particular in the Bow River Basin (Fig. 5b). This led to a large negative bias in precipitation. Performances were strongly improved with *CaPA 10 km New* at the same horizontal resolution (Fig. 7b). Cumulative precipitation greater than 200 mm was better captured but *CaPA 10 km New* still had a negative bias, which was removed with *CaPA 2.5 km* and *CaPA 1.0 km*. Overall, *CaPA 2.5 km* showed the best performance with a lower bias and RMSE, and higher correlation coefficient (Fig. 7c). Compared to *CaPA 2.5 km*, *CaPA 1.0 km* tended to overestimate cumulative precipitation greater than 200 mm for several stations of the Bow River Basin, which led to a slight positive bias.

Improved performance in estimating cumulative precipitation during the flood is not sufficient alone for accurate hydrological simulations, and the precipitation forcing should also reproduce the 6-h precipitation amounts well. Figure 8 uses quantile-quantile (QQ) plots to compare the distribution of observed and analysed precipitation for three datasets (*CaPA 10 km New*, *CaPA 2.5 km* and *CaPA 1.0 km*) and for the three main river basins in southern Alberta. As in Fig. 7, analysed precipitation is derived from the leave-one out method. The concordance correlation coefficient (Lawrence and Lin 1989), RC, is used to estimate the agreement between analyzed and observed 6-h precipitation amounts. RC ranges from -1 to 1. 1 (-1) indicates perfect concordance (discordance) whereas 0 indicates no correlation. Over the Bow River Basin, all datasets reproduced the distribution of 6-h precipitation amounts well, except for amounts above 60 mm. For this basin, the best performance was obtained with *CaPA 1.0 km* (especially over 40 mm). The same conclusion can be made for the Oldman River Basin where *CaPA 10 km New* and *CaPA 2.5 km* underestimated the 6-h precipitation depths greater than 35 mm. Finally, the three version of CaPA has similar performance over the Red Deer River Basin, where no values greater than 40 mm were observed. Overall, Fig. 8 illustrates the added value of precipitation analysis at the kilometre scale for better capturing the intensity of extreme mountain precipitation that may be important for hydrological simulations.

3.3 Hydrological simulations

Initial snow and soil conditions from the *OPL* and *SND* simulations were used in combination with the atmospheric forcing and the QPE products at different resolutions to provide initial and boundary conditions for eight hydrological simulations of

Hydrol. Earth Syst. Sci. Discuss., https://doi.org/10.5194/hess-2019-152
Manuscript under review for journal Hydrol. Earth Syst. Sci.
Discussion started: 23 April 2019

the flooding event over 18 June to 25 June 2013 (Table 4). These simulations were evaluated using discharge measurements from stations on Jumpingpound Creek, Elbow River and Highwood River (Fig. 2). Figure 9 shows the percent bias (PBIAS) of the simulated streamflow volumes for all eight hydrological simulations of the flood, against observed discharge volumes from 20 June 0 UTC to 25 June 0 UTC for different hydrometric stations in our catchments of interest. PBIAS is used to assess the simulation's overall water budget fit during the flooding event: a negative (positive) value denotes a general tendency to under- (over-)estimate streamflow (discharge) volume during the flooding event.

Figure 9 shows a strong underestimation of flood discharge volume for all three gauging locations (station 05BH015 for Jumpingpound Creek, station 05BJ010 for the Elbow River and station 05BL024 for the Highwood River) in simulation *10km_Def_OPL* using initial conditions from the *OPL* run. This underestimation was also observed for all other hydrometric stations shown in Fig. 9 and is consistent with the general underestimation of precipitation in *CaPA 10 km Def* over the foothills and the mountainous part of these basins (Fig. 5b and 7a). Including additional stations and keeping the same resolution in the precipitation analysis (experiment *10km_New_OPL*) leads to a reduction of the negative bias in flood discharge volume. For example, at the outlet of the Elbow River (station 05BJ010), PBIAS decreased from -56% with *10km_Def_OPL* to -24% with *10km_New_OPL*. Increasing the horizontal resolution of the precipitation analysis and of the atmospheric forcing from 10 to 2.5 km (experiments *2.5km_OPL*) brought additional improvements and contributed to reducing the negative PBIAS for discharge at these three river gauging stations. Finally, the *1.0km_OPL* simulation gave similar results with to that of *2.5km_OPL* for these hydrometric stations

The four simulations using initial conditions from the *OPL* run all show an underestimation of the flood discharge volume for gauged sites in three river basins, especially for the Elbow River (-20% in experiment *1.0km_OPL*) and the Highwood River (-28% in experiment *1.0km_OPL*). This may be explained by the underestimation of initial SWE in the basin headwaters in the *OPL* simulation as shown in Fig. 4. For this reason, the *SND* simulation, which incorporates SNODAS SWE to estimate peak snow accumulation, was considered as an alternative to obtain initial snow and soil conditions. Figure 9 shows that this substitution has no impact on hydrological simulations for Jumpingpound Creek as no snow was present in this drainage basin on 18 June 2013 in either simulation (Fig. 4). In contrast, the *SND* simulation with SNODAS-informed initial conditions improved the estimation of flood volume for the Highwood River (station 05BL024) in all simulations with a decrease in the negative bias and nearly unbiased estimates from the *2.5km_SND* and *1.0km_SND* simulations. For the Elbow River, results are different and using *SND* simulations led to an overestimation of the flood volume in all the experiments using the CaPA analysis with additional stations. It should be noted that the SNODAS analysis overestimated SWE close to peak accumulation at the snow pillow located in the headwaters of the Highwood River Basin (Fig. 4). This overestimation of flood discharge volume when using run *SND* was also evident when simulations were compared to observations from the hydrometric stations located in the headwaters of the river basins, station 05BJ004 for the Elbow River and station 05BL019 for the Highwood River.

Hydrol. Earth Syst. Sci. Discuss., https://doi.org/10.5194/hess-2019-152
Manuscript under review for journal Hydrol. Earth Syst. Sci.
Discussion started: 23 April 2019

The streamflow discharge hydrographs during the flood are shown in Fig. 10 for two stations on the Elbow River and in Fig. 11 for two stations on the Highwood River. For each river basin, one station located in the headwater of the catchment and one near the outlet were chosen for analysis. These figures compare the evolution of basin-averaged SWE, basin-averaged cumulated precipitation and streamflow for four GEM-Hydro simulations: *10km_Def_OPL*, *10km_Def_SND*, *1.0km_OPL*, *1.0km_SND*. The filled area on the hydrographs (Fig. 10d, f and Fig. 11d, f) illustrates the impact of using initial conditions from run *SND* instead of run *OPL* for a given meteorological forcing. For all stations, the *10km_Def_OPL* and *10km_Def_SND* simulations failed to capture streamflow dynamics and strongly underestimated the peak flow. Improved results were obtained using the precipitation analysis and the meteorological forcing at 1 km. For the Elbow River (Fig. 10), simulated peak flow was still underestimated with the *1.0km_SND* simulation providing the best results in terms of magnitude. It also gives the best results in terms of timing but still remains late compared to the hydrometric observations (5h and 6h at station 05BJ004 and 05BJ010, respectively). While very little snow is present in simulations using the *OPL* simulation for initial conditions, the decrease in basin-averaged snow mass between 18 and 25 June 2013 reached -62% in the *1.0km_SND* simulation and -56% in the *10km_Def_SND* simulation at station 05BJ004. For the Highwood River (Fig. 11), the *1.0km_SND* simulation overestimated the peak flow at both stations. This overestimation reached 59 % at station 05BL019 (Fig. 11f). The basin draining to this station experienced both intense precipitation and rapid snowmelt on 20 June 2013. The timing of the peak flow was delayed by 11 and 14 hours in *1.0km_SND* and *1.0km_OPL* simulations respectively.

The delay in simulated peak flow is found at the outlets of the Elbow River and the Highwood River for all combinations of initial snow conditions and QPE. This suggests that uncertainties in modelling of river routing with WATROUTE potentially affects the simulations. In particular, erosion and changes in river channels were reported for many rivers impacted by the June 2013 flood (Pomeroy et al., 2016b) and a shift from sub-surface to overland flow was noted (Pomeroy et al., 2016a; Fang and Pomeroy, 2016), suggesting that the default routing parameters used in WATROUTE may not be suitable for this extreme event. To test this assumption, additional routing experiments were made using the *1.0km_SND* and *1.0km_OPL* simulations that benefited from the most accurate precipitation forcing (Fig. 7 and 8). The Manning's coefficients over the GEM-Hydro simulation domain were successively decreased by 10, 20, 30 and 40% and the timing of the simulated peak flow compared to discharge observations. Figure 12 compared the hydrographs obtained in the default configuration with those where Manning coefficients were reduced by 30 % because this gave the best peak flow simulations. For the Elbow River (Fig. 12a and b), adjusting the Manning coefficients allowed GEM-Hydro to better capture the rapid increase in streamflow observed at both stations. It also improved the timing of the peak flow, for example the delays were reduced from + 10 (+ 5) hours to +1 (-2) hours in the *1.0km_OPL* (*1.0km_SND*) simulations at station 05BJ010. The magnitude of the peak flow was only slightly impacted by decreasing Manning's coefficient. A similar improvement in the simulated timing of the peak flow was found for the Highwood River (Fig. 12d) however this came at a cost of degraded peak flow estimation; the *1.0km_SND* simulation with updated Manning's coefficients overestimated the magnitude of the peak flow

by 33% compared to 14% in the default configuration. An early and overestimated peak flow was also found in the headwaters of the Highwood River Basin (Fig. 12c) with the *1.0km_SND* simulation when using updated Manning's coefficients. This shows that simple, spatially uniform adjustment of Manning's coefficients is not sufficient to capture the peak flow timing and magnitudes observed at various hydrometric stations. This is likely due to the substantial spatial and temporal variability in runoff, storage and channel processes (Fang and Pomeroy, 2016) and that such a hydraulic calibration is necessarily combined with other sources of uncertainties in the timing and magnitude of intense precipitation and snowmelt in the land surface scheme, and in the other hydraulic parameters of the routine scheme such as channel width and geometry.

4. Discussion

This paper has examined the ability of the GEM-Hydro hydrological modelling platform to simulate streamflows during the June 2013 Flood in southern Alberta. This is the first time GEM-Hydro has been evaluated in this region of Canada, which is characterized by a transition from headwaters in the complex topography of the Canadian Rockies towards downstream plains. The simulation of this extreme event offers insights into the key factors governing the prediction skill of flooding events in this region and the associated modelling challenges.

4.1 Quantitative Precipitation Estimation

This study used four QPE products to assess how QPE accuracy influences GEM-Hydro simulations. The QPE products were generated using the Canadian Precipitation Analysis (CaPA) system with varying station density and different horizontal resolutions of the GEM precipitation background. The results of this study show that the QPE product that most resembles the CaPA product that was generated in operations at ECCC at the time of the flood (10-km grid spacing, SYNOP stations only) led to a strong underestimation of precipitation in the mountainous parts of the region and a systematic underestimation of the flood volume in the Elbow and Highwood River catchments. This version of CaPA was used to evaluate precipitation simulated by atmospheric models during the June 2013 Flood in several previous studies (Liu et al., 2016; Teufel et al., 2017). Including additional stations from university and provincial networks led to significant improvements in the 10-km precipitation analysis for the headwaters that received the largest amount of precipitation during the flood with a positive impact on the hydrological response simulated by GEM-Hydro. This illustrates the continuous need to include stations from additional networks in operational precipitation analysis systems used for hydrological modelling as already discussed in several studies (Lespinas et al., 2015; Soci et al., 2016; Fortin et al., 2018). This need is critical in the mountainous regions of Western Canada where the network of stations used in the operational version of CaPA (Fortin et al., 2018) is scarce with stations mainly located at low elevation valley bottoms. Radar data were not considered in our study since Kochtubajda et al. (2016) showed that these data were affected by attenuation during the heavy precipitation periods of the flooding event and produced rate and accumulation lower than gauges estimates in mountainous areas.

Increasing the resolution of the GEM precipitation background from 10 km to kilometre scales (2.5 and 1 km) improved the accuracy of the final QPE products in terms of cumulative precipitation as well as the intensity of extreme precipitation during the flooding event. Streamflow simulated by GEM-Hydro benefited from these improvements in forcing data. The largest difference was found in moving from 10-km QPE to the 2.5 km QPE which invoked precipitation forcing data from a convection-permitting NWP system. Li et al. (2017) and Milrad et al. (2017) have shown that atmospheric models at such resolution were required to capture the spatial and temporal variability of extreme precipitation during the June 2013 flooding event. This has also been shown in other mountainous regions (e.g. Richard et al., 2007; Weusthoff et al., 2010; Rasmussen et al., 2011). The results shown here confirm that improving the realism of the precipitation model in complex terrain also improves the precipitation analysis. This shows the potential to improve hydrological forecasting by using the latest operational version of CaPA running at 2.5 km over Canada (Fortin et al., 2018). On the other hand, only marginal improvements in the intensity of extreme precipitation and slight degradation of cumulative precipitation predictions were found when increasing the resolution of the precipitation model from 2.5 km to 1 km. Theses findings are in agreement with Pontoppidan et al. (2017) who showed only minor improvements from 3 km to 1 km in atmospheric simulations of an intense precipitation event in Western Norway. Further evaluations are required in the mountains of Western Canada to clearly assess the benefits and limitations of a 1-km precipitation analysis. In this context, further developments are also required in CaPA to better account for the effect of complex topography in the optimal interpolation scheme (Daly, et al., 1994; Gottardi et al., 2012).

4.2 Initial snow conditions

The June 2013 Flood was characterized by rain falling on a late-lying snowpack at high elevations inducing rain-on-snowmelt and enhancing runoff generation such that there was more runoff than storm precipitation (Fang and Pomeroy, 2016). The results shown here confirm the impact of initial snow conditions on simulated flood volume and dynamics, in agreement with previous studies (Pomeroy et al., 2016a; Teufel et al. 2017) and illustrate the challenge of obtaining realistic information on snow conditions in the Canadian Rockies. Indeed, the first set of hydrological simulations used initial snow conditions taken from an open-loop simulation of GEM-Surf and presented a systematic underestimation of flood volume in GEM-Hydro simulations with all QPE products. This is mainly due to the absence of snow in the high elevation headwaters at the time of the flood, which resulted from a strong and systematic underestimation of winter snow accumulation. These results are consistent with the earlier findings of Carrera et al. (2010) and Separovic et al. (2014) and are mainly explained by an underestimation of mountain winter precipitation simulated by GEM at 10-km grid spacing (Schirmer and Jamieson, 2015). This illustrates the challenge of obtaining accurate snow simulations in mountainous terrain when relying on precipitation forcing made of successive forecasts (e.g. Bellaire et al., 2011; Vionnet et al. 2016). In addition, GEM-Surf at 1-km grid spacing does not simulate key processes such as wind-induced and gravitational snow transport (e.g. Bernhardt and Schulz, 2010; Vionnet et al., 2014; Musselman et al., 2015) or the effect of slope on incoming radiation (e.g. Oliphant et

al., 2003) that influence winter snow accumulation and runoff generation in mountainous catchment (DeBeer and Pomeroy, 2017; Brauchli et al., 2017).

The insertion of SWE data from the SNODAS operational snow analysis system (Barrett, 2003) near the time of peak snow accumulation was tested to correct the negative bias in winter snow accumulation and to obtain more realistic snow and soil initial condition at high elevation. GEM-Hydro simulations including SNODAS SWE showed contrasting results. In particular, the overestimation of flood volume found at the stations located in the headwaters of the Elbow and Highwood River basins suggests an overestimation of basin-average SWE prior to the flood. This is in agreement with the overestimation of SWE close to peak accumulation reported using snow pillows observations at high elevations in these basins. Teufel et al. (2017) also found an overestimation of daily simulated streamflow when using initial snow conditions from SNODAS in their hydrological simulations of the June 2013 flood. In a recent study, Lv et al. (in review, WRR) reported a strong overestimation of SNODAS SWE in sub-alpine forest elevations in the Canadian Rockies. They have also found a poor agreement in open alpine environments due to missing wind-induced snow redistribution processes in SNODAS, similarly to the results obtained by Clow et al. (2012) in the Colorado Rocky Mountains. Our results show that there is a strong need for the development of an improved snow analysis product in the Canadian Rockies that can be used for hydrological applications.

4.3 Model uncertainties and limitations

The analysis of the hourly flood hydrograph simulations highlights the crucial roles of precipitation forcing, initial snow conditions and hydraulic parameter selection in accurate flood simulations. Using the 1-km QPE as driving data, a reduction of Manning's equation coefficients by 30% compared to the default values in GEM-Hydro was required to capture the timing of peak flow at the outlets of the Elbow River and Highwood River. For these two rivers, the timing of the peak flow was more sensitive than the magnitude to adjustment of Manning's equation coefficients. In a recent study, Lin et al. (2018) demonstrated that the flood prediction skill of the US National Water Model (Maidment, 2017) is affected by flow velocity in the river network. The results shown here suggest that the set of Manning's coefficients used in the default version of GEM-Hydro would benefit from specific selection to individual rivers in southern Alberta. The channel area in WATROUTE, that controls whether flow is contained in the main channel or the overbank part, may need to be selected by river as well. Calibration these parameters based on historical data may not be suitable for an extreme event such as the June 2013 flood when major changes occurred in the geometry of the riverbeds (Pomeroy et al., 2016b), but parameter selection from hydraulic characteristics measured by the Water Survey of Canada and from remote sensing and field surveys is an alternative parameterisation methodology used at multiple scales in the region (Pomeroy et al., 2013).

In addition to uncertainties in the routing scheme parameters, GEM-Hydro has several limitations in its SVS land surface scheme for application to mountain and cold-region hydrology. SVS uses a 1-layer snowpack scheme to simulate the snow

cover evolution over bare ground and low vegetation and below high-vegetation. Due to simplification in the representation of water flow through flat and sloping snowpacks, internal snowpack coupled phase change and energy exchange and the crude turbulent transfer scheme employed, such a scheme will be challenged by rain-on-snow events (Würzer et al. 2016) and by the occurrence of preferential flow pathways, layering and refreezing in snowpacks (Leroux and Pomeroy, 2018; 2019). SVS snow neglects surface layer snow energetics, canopy snow interception, melt, unloading and sublimation, and blowing snow transport and sublimation processes which are necessary for successful simulations of snowpacks in this region (Pomeroy et al., 2008; Fang et al., 2013; Pomeroy et al., 2016a; 2016c). SVS considers all topography to be flat meaning that its snowpack energetics in mountains will vary from those observed not only in magnitude but in sign (Pomeroy et al., 2003; Ellis et al., 2013). In addition, SVS does not simulate soil freezing and its strong impact on infiltration to frozen soils (e.g. Zhao and Gray, 1999; Gray et al., 2001) and on hillslope hydrological processes (Carey et al., 2007). Pomeroy et al. (2016b) and Teufel et al. (2017) suggested that the presence of frozen soil at high elevations and in valley bottoms modified snowmelt infiltration and contributed to the runoff generation during the June 2013 flooding event. To overcome some of these limitations, ECCC is currently working on the development of a new version of SVS that will solve the heat diffusion equation in the soil including freeze/thaw processes and include a more advanced multi-layer snowpack scheme (Decharme et al., 2016).

5. Conclusions

This study aims to evaluate the ability of the GEM-Hydro modelling platform to simulate (in hindcast mode) hydro-meteorological conditions during the June 2013 flood in southern Alberta and to identify the main factors important for accurately reproducing the flood dynamics. Toward this goal, a 1-km resolution configuration of the model was used in a way similar to the standard coarser resolution configurations used at ECCC. The GEM atmospheric model was used in combination with the CaPA precipitation analysis system to generate several QPE products for the flood with varying station densities (especially in the mountainous part of the catchments) and different horizontal resolutions (10, 2.5 and 1 km). In addition to the QPE products, two sets of initial snow conditions were also considered to assess their impact on hydrological simulations in the Elbow and Highwood river basins, which were strongly impacted during the flooding event. Major conclusions of the model evaluation are summarized below.

- The increase in the number of stations integrated in CaPA as well as the use of a modelled precipitation at the kilometre scale (2.5 and 1 km) greatly improved QPE accuracy in the mountainous part of the catchments, both in terms of cumulative and extreme values of precipitation. This translates into improvements of the simulation of the flood volume by GEM-Hydro, highlighting the primary and critical role of precipitation input in accurate flood prediction.
- Hydrological simulations starting with almost no snowpack at high-elevations led to a systematic underestimation of flood volume and peak flow for all QPE driving data. The insertion of SNODAS SWE data near the time of peak

snow accumulation provided initial conditions with substantial snowpacks and coverage at high-elevation. The use of SNOWDAS SWE led to contrasting abilities to simulate flood discharge volumes and a consistent overestimation in the mountainous part of the catchments when combined with the most accurate QPE. These results confirm the importance of accurate initial snow conditions for accurate spring and early summer flood simulation in this region and shows the need for more accurate snow products in the Canadian Rockies.

- The model suffers from poor prediction skill for the timing of the peak flow with a systematic delay. By conducting a series of model sensitivity tests, it was shown that improved flood peak timing can be obtained by tuning Mannings's coefficient in the routing scheme. However, uniform tuning of this parameter was not successful in estimating both peak flow timing and magnitude. This clearly highlights large uncertainties in routing parameters during extreme events and the need for revised and specific routing parameters for the rivers of this region.

This study is the first evaluation of the flood prediction skill of GEM-Hydro in mountainous terrain and downstream. The hydrological simulations analysed here were driven by QPE products obtained with a precipitation analysis system. The results are promising but further evaluation is required for such extreme events with GEM Hydro driven by deterministic or ensemble precipitation forecast from NWP systems. GEM-Hydro as a hydrological forecasting system is currently being implemented by ECCC in Western Canada. Improvements of the forecasting system are can be expected with future development of a new reference snow product for the Canadian Rockies and the development of a new version of the land surface scheme SVS to better simulate the snow and frozen ground processes impacting cold regions hydrology.

Data availability

The CaPA and GEM data at different resolutions are publicly available on the Federated Research Data Repository (Vionnet et al., 2019).

Authors contribution

VV, VF and JP designed the study. VV run the numerical experiments with GEM, CaPA, and GEM-Hydro and was responsible for the preparation of the manuscript. GR designed the CaPA experiments. VF, NG and EG contributed to the preparation of the experiments with GEM-Hydro and the analysis of the results. MA provided the latest version of the land-surface scheme SVS and contributed to the preparation of configuration of SVS used in this paper. All authors contributed to the preparation of the manuscript.

Competing interest

The authors declare that they have no conflict of interest.

Acknowledgements

This study was supported by the Global Water Future project funded by the Canada First Research Excellence Fund. Support from the Canada Research Chairs, NSERC, Alberta Innovates and Global Institute for Water Security is gratefully acknowledged. Milena Dimitrijevic (ECCC), Manon Faucher (ECCC) and Dorothy Durnford (ECCC) are thanked for their helpful contribution with GEM and GEM-Hydro. Special thanks to Nic Wayand (U. Washington) and Samantha Hussey (ECCC) for providing precipitation, snow and discharge data.

References

Alavi, N., S. Bélair, V. Fortin, S. Zhang, S. Z. Husain, M. L. Carrera, and M. Abrahamowicz. Warm Season Evaluation of Soil Moisture Prediction in the Soil, Vegetation, and Snow (SVS) Scheme. J. Hydrometeorol. 17 (8): 2315–32, 2016,

Barrett, A. P. National operational hydrologic remote sensing center snow data assimilation system (SNODAS) products at NSIDC. National Snow; Ice Data Center, Cooperative Institute for Research in Environmental Sciences Boulder, CO, 2003

Bellaire, S., J.B. Jamieson, and C. Fierz. Forcing the snow-cover model SNOWPACK with forecasted weather data. The Cryosphere 5 (4). 1115–25, https://doi.org/10.5194/tc-5-1115-2011, 2003

Bernhardt, M., and K. Schulz. SnowSlide: A simple routine for calculating gravitational snow transport. Geophy. Res. Let. 37 (11), https://doi.org/10.1029/2010GL043086, 2010

Bernier, N., S. Bélair, B. Bilodeau, and L. Tong. Near-surface and land surface forecast system of the Vancouver 2010 Winter Olympic and Paralympic Games. J. Hydrometeorol. 12 (4): 508–30, https://doi.org/10.1175/2011JHM1250.1, 2011

Brasnett, B. A Global Analysis of Snow Depth for Numerical Weather Prediction. J. Appl. Meteorol. 38 (6): 726–40, https://doi.org/10.1175/1520-0450(1999)038<0726:AGAOSD>2.0.CO;2, 1999

Brauchli, T., E. Trujillo, H. Huwald, and M. Lehning. Influence of Slope-Scale Snowmelt on Catchment Response Simulated With the Alpine3D Model. Water Resour. Res. 53 (12). 10723–39, 2017, https://doi.org/10.1002/2017WR021278

Carey, S. K., Quinton, W. L. and Goeller, N. T. Field and laboratory estimates of pore size properties and hydraulic characteristics for subarctic organic soils. Hydrol. Process., 21: 2560-2571, https://doi.org/10.1002/hyp.6795, 2007

Caron, J.-F., T. Milewski, M. Buehner, L. Fillion, M. Reszka, S. Macpherson, and J. St-James. Implementation of deterministic weather forecasting systems based on ensemble–variational data assimilation at Environment Canada. Part II: The regional system. Mon. Wea. Rev. 143 (7): 2560–80, https://doi.org/10.1175/MWR-D-14-00353.1, 2015

Carrera, M., S. Bélair, V. Fortin, B. Bilodeau, D. Charpentier, and I. Doré. Evaluation of snowpack simulations over the Canadian Rockies with an experimental hydrometeorological modeling system. J. Hydrometeorol. 11 (5): 1123–40, https://doi.org/10.1175/2010JHM1274.1, 2010

Chow, V. T., 1959: Open-channel Hydraulics, McGraw-Hill, New York, 680 pp.

Clark, M. P., Y. Fan, D. M. Lawrence, J. C. Adam, D. Bolster, D. J. Gochis, R. P. Hooper, et al. Improving the representation of hydrologic processes in Earth System Models. Wat. Resour. Res. 51 (8): 5929–56, https://doi.org/10.1002/2015WR017096, 2015

Clow, D. W., L. Nanus, K. L. Verdin, and J. Schmidt. Evaluation of SNODAS snow depth and snow water equivalent estimates for the Colorado Rocky Mountains, USA. Hydrol. Proc. 26 (17). 2583–91. https://doi.org/10.1002/hyp.9385, 2012

Côté, J., S. Gravel, A. Méthot, A. Patoine, M. Roch, and A. Staniforth. The operational CMC–MRB global environmental multiscale (GEM) model. Part I: Design considerations and formulation. Mon. Wea. Rev. 126 (6): 1373–95. https://doi.org/10.1175/1520-0493(1998)126<1373:TOCMGE>2.0.CO;2, 1998

Daly, C., R. P. Neilson, and D. L. Phillips. A Statistical-Topographic Model for Mapping Climatological Precipitation over Mountainous Terrain. J. Appl. Meteorol. 33 (2): 140–58. https://doi.org/10.1175/1520-0450(1994)033<0140:ASTMFM>2.0.CO;2, 1994

DeBeer, C.M., and J.W. Pomeroy. Simulation of the Snowmelt Runoff Contributing Area in a Small Alpine Basin. Hydrol. Earth Sys. Sci. 14 (7): 1205. https://doi.org/10.5194/hess-14-1205-2010, 2010

DeBeer C.M., Pomeroy J.W. Influence of snowpack and melt energy heterogeneity on snow cover depletion and snowmelt runoff simulation in a cold mountain environment, J. Hydrol., 553: 199 – 213, https://doi.org/10.1016/j.jhydrol.2017.07.051, 2017

Decharme, B., Alkama, R., Douville, H., Becker, M., & Cazenave, A. Global evaluation of the ISBA-TRIP continental hydrological system. Part II: Uncertainties in river routing simulation related to flow velocity and groundwater storage. J. Hydrometeorol., 11(3), 601-617. https://doi.org/10.1175/2010JHM1212.1, 2010

Decharme, B., E. Brun, A. Boone, C. Delire, P. Le Moigne, and S. Morin. Impacts of snow and organic soils parameterization on northern Eurasian soil temperature profiles simulated by the ISBA land surface model. The Cryosphere 10 (2): 853–77. https://doi.org/10.5194/tc-10-853-2016, 2016

Durnford, D., V. Fortin, G. C. Smith, B. Archambault, D. Deacu, F. Dupont, S. Dyck, et al. Toward an Operational Water Cycle Prediction System for the Great Lakes and St. Lawrence River. B. Am. Meteorol. Soc. 99 (3): 521–46. https://doi.org/10.1175/BAMS-D-16-0155.1, 2018

Ellis C.R., Pomeroy J.W., Link T.E. Modelling Increases in Snowmelt Yield and Desynchronization Resulting from Forest Gap-Thinning Treatments in a Northern Mountain Headwater Basin, Wat. Resour. Res., 49(2): 936 - 949. https://doi.org/10.1002/wrcr.20089, 2013

Fang X, Pomeroy JW, Ellis CR, MacDonald MK, DeBeer CM, Brown T. Multi-Variable Evaluation of Hydrological Model Predictions for a Headwater Basin in the Canadian Rocky Mountains, Hydrol. Earth Sys. Sci, *17*(4): 1635 - 1659. https://doi.org/10.5194/hess-17-1635-2013, 2013

Fang, X., and J.W. Pomeroy. Impact of Antecedent Conditions on Simulations of a Flood in a Mountain Headwater Basin. Hydrol. Proc. 30 (16): 2754–72. https://doi.org/10.1002/hyp.10910, 2016

Fortin, V., G. Roy, N. Donaldson, and A. Mahidjiba. Assimilation of radar quantitative precipitation estimations in the Canadian Precipitation Analysis (CaPA). J. Hydrol. 531: 296–307, https://doi.org/10.1016/j.jhydrol.2015.08.003, 2015

Fortin, V., G. Roy, T. Stadnyk, K. Koenig, N. Gasset, and A. Mahidjiba. Ten Years of Science Based on the Canadian Precipitation Analysis: A CaPA System Overview and Literature Review. Atmos.-Ocean. 1–19, https://doi.org/10.1080/07055900.2018.1474728, 2018

Gaborit, E., V. Fortin, X. Xu, F. Seglenieks, B. Tolson, L. M. Fry, T. Hunter, F. Anctil, and A. D. Gronewold. A hydrological prediction system based on the SVS land-surface scheme: efficient calibration of GEM-Hydro for streamflow simulation over the Lake Ontario basin. Hydrol. Earth Syst. Sci. 21 (9): 4825–39., https://doi.org/10.5194/hess-21-4825-2017, 2017

Girard, C., A. Plante, M. Desgagné, R. McTaggart-Cowan, J. Côté, M. Charron, S. Gravel, et al. Staggered vertical discretization of the Canadian Environmental Multiscale (GEM) model using a coordinate of the log-hydrostatic-pressure type. Mon. Wea. Rev. 142 (3): 1183–96, https://doi.org/10.1175/MWR-D-13-00255.1, 2014

Gochis, D.J., W. Yu, and D.N. Yates. The WRF-Hydro Model Technical Description and User's Guide, Version 3.0, NCAR Technical Document, 120 pp, 2015

Gottardi, F., C. Obled, J. Gailhard, and E. Paquet. Statistical Reanalysis of Precipitation Fields Based on Ground Network Data and Weather Patterns: Application over French Mountains. J. Hydrol. 432. 154–67, https://doi.org/10.1016/j.jhydrol.2012.02.014, 2012

Gray D.M., Toth B., Pomeroy J.W., Zhao L, Granger R.J. Estimating Areal Snowmelt Infiltration into Frozen Soils, *Hydrol. Proc., 15* 3095 – 3111, https://doi.org/10.1002/hyp.320, 2001

GWF project. Global Water Futures: Annual Progress Report 2017-2018. University of Saskatchewan. https://gwf.usask.ca/documents/GWF_Annual-Report_2017-2018.pdf., 2018

Husain, S. Z., N. Alavi, S. Bélair, M. Carrera, S. Zhang, V. Fortin, M. Abrahamowicz, and N. Gauthier. The multibudget Soil, Vegetation, and Snow (SVS) scheme for land surface parameterization: Offline warm season evaluation. J. Hydrometeorol. 17 (8): 2293–2313., https://doi.org/10.1175/JHM-D-15-0228.1, 2016

Kochtubajda, B., R.E. Stewart, S. Boodoo, J.M. Thériault, Y. Li, A. Liu, C. Mooney, R. Goodson, and K. Szeto. The June 2013 Alberta catastrophic flooding event–part 2: fine-scale precipitation and associated features. Hydrol. Proc. 30 (26). Wiley Online Library: 4917–33, https://doi.org/10.1002/hyp.10855, 2016

Kouwen, N. WATFLOOD/WATROUTE Hydrological model routing & flow forecasting system. Department of Civil Engineering, University of Waterloo, Waterloo, Ontario, Canada, 2010

Lawrence, I., and Kuei Lin. A Concordance Correlation Coefficient to Evaluate Reproducibility. Biometrics. JSTOR, 255–68, 1989

Lehner, B., K. Verdin, and A. Jarvis. New Global Hydrography Derived from Spaceborne Elevation Data. Eos, Transactions American Geophysical Union 89 (10): 93–94, https://doi.org/10.1029/2008EO100001, 2008

Leroux N.R., Pomeroy J.W. Modelling capillary hysteresis effects on preferential flow through melting and cold layered snowpacks, Adv. Wat. Resour., 107(-): 250 – 264, https://doi.org/10.1016/j.advwatres.2017.06.024, 2017

Leroux N.R., Pomeroy J.W. Simulation of Capillary Overshoot in Snow Combining Trapping of the Wetting Phase with a Non-Equilibirum Richards Equation Model, Water Resour. Res., 55(1): 236-248 https://doi.org/10.1029/2018WR022969, 2019

Leroyer, S., S. Bélair, L. Spacek, and I. Gultepe. Modelling of Radiation-Based Thermal Stress Indicators for Urban Numerical Weather Prediction. Urban Climate 25: 64–81, https://doi.org/10.1016/j.uclim.2018.05.003, 2018

Lespinas, F., V. Fortin, G. Roy, P. Rasmussen, and T. Stadnyk. Performance evaluation of the Canadian Precipitation Analysis (CaPA). J. Hydrometeorol., 16 (5): 2045–64, https://doi.org/10.1175/JHM-D-14-0191.1, 2015

Li, Y., K. Szeto, R. E. Stewart, J. M. Thériault, L. Chen, B. Kochtubajda, A. Liu, et al. A numerical study of the June 2013 flood-producing extreme rainstorm over southern Alberta. J. Hydrometeorol. 18 (8): 2057–78, https://doi.org/10.1175/JHM-D-15-0176.1, 2017

Lin, P., L. J. Hopper Jr, Z.-L. Yang, M. Lenz, and J. W. Zeitler. Insights into hydrometeorological factors constraining flood prediction skill during the May and October 2015 Texas Hill Country flood events. J. Hydrometeorol. 19 (8): 1339–61, https://doi.org/10.1175/JHM-D-18-0038.1, 2018

Liu, A.Q., C. Mooney, K. Szeto, J.M. Thériault, B. Kochtubajda, R.E. Stewart, R. Boodoo S .and Goodson, Y. Li, and J. Pomeroy. The June 2013 Alberta catastrophic flooding event: Part 1—climatological aspects and hydrometeorological features. Hydrol. Process. 30 (26): 4899–4916, https://doi.org/10.1002/hyp.10906, 2016

Mahfouf, J.-F., B. Brasnett, and S. Gagnon. A Canadian precipitation analysis (CaPA) project: Description and preliminary results. Atmos.-Ocean 45 (1): 1–17, https://doi.org/10.3137/ao.v450101, 2007

Maidment, D. R. Conceptual Framework for the National Flood Interoperability Experiment. J. Am. Water Resour. As. 53 (2): 245–57, https://doi.org/10.1111/1752-1688.12474, 2017

Milbrandt, J. A., S. Bélair, M. Faucher, M. Vallée, M. L. Carrera, and A. Glazer. The pan-Canadian high resolution (2.5 km) deterministic prediction system. Weather and Forecast. 31 (6): 1791–1816, https://doi.org/10.1175/WAF-D-16-0035.1, 2016

Milrad, S. M., J. R. Gyakum, and E. H. Atallah. A meteorological analysis of the 2013 Alberta flood: Antecedent large-scale flow pattern and synoptic–dynamic characteristics. Mon. Wea. Rev. 143 (7): 2817–41, https://doi.org/10.1175/MWR-D-14-00236.1, 2015

Milrad, S. M., K. Lombardo, E. H. Atallah, and J. R. Gyakum. Numerical Simulations of the 2013 Alberta Flood: Dynamics, Thermodynamics, and the Role of Orography. Mon. Wea. Rev. 145 (8): 3049–72, https://doi.org/10.1175/MWR-D-16-0336.1, 2017

Morrison, H., and J. A. Milbrandt. Parameterization of cloud microphysics based on the prediction of bulk ice particle properties. Part I: Scheme description and idealized tests. J. Atmos. Sci. 72 (1): 287–311, https://doi.org/10.1175/JAS-D-14-0065.1, 2015

Musselman, K.N., J.W. Pomeroy, R.L.H. Essery, and N. Leroux. Impact of windflow calculations on simulations of alpine snow accumulation, redistribution and ablation. Hydrol. Proc. 29 (18). Wiley Online Library: 3983–99, https://doi.org/10.1002/hyp.10595, 2015

Oliphant, A.J., R.A. Spronken-Smith, A.P. Sturman, and I.F. Owens. Spatial variability of surface radiation fluxes in mountainous terrain. J. Appl. Meteorol. 42 (1): 113–28, https://doi.org/10.1175/1520-0450(2003)042<0113:SVOSRF>2.0.CO;2, 2003

Pomeroy J.W., Gray D.M., Shook K.R., Toth B., Essery R.L.H., Pietroniro A., Hedstrom N. An Evaluation of Snow Accumulation and Ablation Processes for Land Surface Modelling, Hydrol. Proc., 12(-): 2339 – 2367, https://doi.org/10.1002/(SICI)1099-1085(199812)12:15<2339::AID-HYP800>3.0.CO;2-L, 1998

Pomeroy J.W., Toth B., Granger R. J., Hedstrom N. R., Essery R.L.H. Variation in Surface Energetics During Snowmelt in Complex Terrain, J. Hydrometeorol., *4*(4): 702 – 716, https://doi.org/10.1175/1525-7541(2003)004<0702:VISEDS>2.0.CO;2, 2003

Pomeroy J. W., Fang X., Shook K., Whitfied P. H. Predicting in Ungauged Basins Using Physical Principles Obtained Using Deductive, Inductive and Abductive Reasoning Approach, In Putting Prediction in Ungauged Basins into Practice (pp. 43 - 63), 2013

Pomeroy J W., X. Fang, and D. G. Marks. The cold rain-on-snow event of June 2013 in the Canadian Rockies: characteristics and diagnosis. Hydrol. Process. 30 (17). Wiley Online Library: 2899–2914, https://doi.org/10.1002/hyp.10905, 2016a

Pomeroy, J. W., R. E. Stewart, and P. H. Whitfield. The 2013 flood event in the South Saskatchewan and Elk River basins: Causes, assessment and damages. Can. Water Resour.. J. 41 (1-2). Taylor & Francis: 105–17, https://doi.org/10.1080/07011784.2015.1089190, 2016b

Pomeroy J. W., Essery R.L.H., Helgason W.D. Aerodynamic and Radiative Controls on the Snow Surface Temperature, J. Hydrometeorol., 17(-): 2175 – 2189, https://doi.org/10.1175/JHM-D-15-0226.1, 2016

Pontoppidan, M., J. Reuder, S. Mayer, and E. W. Kolstad. Downscaling an Intense Precipitation Event in Complex Terrain: The Importance of High Grid Resolution. Tellus A 69 (1), https://doi.org/10.1080/16000870.2016.1271561, 2017

Rasmussen, R., C. Liu, K. Ikeda, D. Gochis, D. Yates, F. Chen, M. Tewari, et al. High-resolution coupled climate runoff simulations of seasonal snowfall over Colorado: A process study of current and warmer climate. J. Climate 24 (12): 3015–48, https://doi.org/10.1175/2010JCLI3985.1, 2011

Richard, E., A. Buzzi, and G. Zängl. Quantitative precipitation forecasting in the Alps: The advances achieved by the Mesoscale Alpine Programme. *Quat. J. Roy. Met. Soc.* 133 (625): 831–46, https://doi.org/10.1002/qj.65, 2007

Schirmer, M., and B. Jamieson. 2015. Verification of Analysed and Forecasted Winter Precipitation in Complex Terrain. The Cryosphere 9 (2): 587–601, https://doi.org/10.5194/tc-9-587-2015, 2015

Separovic, L., S. Z. Husain, W. Yu, and D. Fernig. High-resolution surface analysis for extended-range downscaling with limited-area atmospheric models. J. Geophys. Res.: Atm. 119 (24). 13–651, https://doi.org/10.1002/2014JD022387, 2014

Soci, C., E. Bazile, F. Besson, and T. Landelius. High-Resolution Precipitation Re-Analysis System for Climatological Purposes. Tellus A 68 (1), https://doi.org/10.3402/tellusa.v68.29879, 2016

Soulis, E. D., Craig, J. R., Fortin, V., & Liu, G. A simple expression for the bulk field capacity of a sloping soil horizon. Hydrol. Proc., 25(1), 112-116, https://doi.org/10.1002/hyp.7827, 2011

Sundqvist, H. A Parameterization Scheme for Non-Convective Condensation Including Prediction of Cloud Water Content. *Q. J. Roy. Meteor. Soc.* 104 (441): 677–90, https://doi.org/10.1002/qj.49710444110, 1978

Teufel, Bernardo, G. T. Diro, K. Whan, S. M. Milrad, D. I. Jeong, A. Ganji, O. Huziy, et al. Investigation of the 2013 Alberta flood from weather and climate perspectives. *Climate Dynamics* 48 (9-10) : 2881–99, doi: 10.1007/s00382-016-3239-8, 2017

Vionnet, V., E. Martin, V. Masson, G. Guyomarc'h, F. Naaim Bouvet, A. Prokop, Y. Durand, and C. Lac. Simulation of Wind-Induced Snow Transport and Sublimation in Alpine Terrain Using a Fully Coupled Snowpack/Atmosphere Model. The Cryosphere 8, https://doi.org/10.5194/tc-8-395-2014, 2014

Vionnet, V., S. Bélair, C. Girard, and A. Plante. Wintertime subkilometer numerical forecasts of near-surface variables in the Canadian Rocky Mountains. Mon. Wea. Rev. 143 (2): 666–86, https://doi.org/10.1175/MWR-D-14-00128.1, 2015

Vionnet, V., I. Dombrowski-Etchevers, M. Lafaysse, L. Quéno, Y. Seity, and E. Bazile. Numerical weather forecasts at kilometer scale in the French Alps: evaluation and application for snowpack modeling. J. Hydrometeorol. 17 (10): 2591–2614, https://doi.org/10.1175/JHM-D-15-0241.1, 2016

Vionnet, V., Fortin, V., Gaborit, E., Roy, G., Abrahamowicz, M., Gasset, N., & Pomeroy, J. W. A multi-scale meteorological dataset of the June 2013 flood in Southern Alberta, Canada [Dataset]. Federated Research Data Repository. https://doi.org/10.20383/101.0130, 2019

Weusthoff, T., F. Ament, M. Arpagaus, and M. W. Rotach. Assessing the benefits of convection-permitting models by neighborhood verification: Examples from MAP D-PHASE. *Mon. Wea. Rev.* 138 (9): 3418–33, https://doi.org/10.1175/2010MWR3380.1, 2010

Würzer, S., T. Jonas, N. Wever, and M. Lehning. 2016. Influence of Initial Snowpack Properties on Runoff Formation During Rain-on-Snow Events. J. Hydrometeorol. 17 (6): 1801–15, https://doi.org/10.1175/JHM-D-15-0181.1, 2016

Zhao, L., and D.M. Gray. Estimating Snowmelt Infiltration into Frozen Soils. Hydrol. Proc. 13 (12-13). Wiley Online Library: 1827–42, https://doi.org/10.1002/(SICI)1099-1085(199909)13:12/13<1827::AID-HYP896>3.0.CO;2-D, 1999

Hydrol. Earth Syst. Sci. Discuss., https://doi.org/10.5194/hess-2019-152
Manuscript under review for journal Hydrol. Earth Syst. Sci.
Discussion started: 23 April 2019

Hydrology and Earth System Sciences
Discussions

Table 1. Summary of GEM model configuration and references for the different physical parameterizations used in the model. The centre of the 3 domains is located at 51.44 N and -114.0 W.

Category	Model	GEM 10 km	GEM 2.5 km	GEM 1 km
Horizontal	Grid spacing (km)	10.0	2.5	1.0
	Grid size	360 × 360	540 × 540	768 × 768
	Domain (km)	3600 × 3600	1350 × 1350	768 × 768
Vertical	Levels numbers	80	62	62
	Lowest levels (m)	40 m (momentum), 20 m (thermodynamics)		
Time	Time step (s)	240	60	30
	Update interval (min)	60	12	12
Physics	Land Surface	ISBA (Belair et al., 2003a,b)		
	Planet Boundary Layer	MoisTKE (Belair et al., 2005)		
	Deep convection	Kain and Fritsh (1990, 1993)[a]		None
	Shallow convection	Kuo-transient scheme (Belair et al., 2005)		
	Cloud Microphysics	Sundqvist (1978)	P3 (Morrison and Milbrandt, 2015)	

[a]parameter settings for KF scheme depend on model resolution

Table 2. Geophysical databases used to generate surface fields for the GEM experiments at different resolutions.

Field	Database	Resolution	Experiments
Orography	U.S. Geological Survey Global 30 arc s elevation dataset (https://lta.cr.usgs.gov/GTOPO30)	30 arc s	GEM 10 km
	Canadian Digital Elevation Data (CDED) over Canada (http://ftp.geogratis.gc.ca/pub/nrcan_rncan/elevation/cdem_mnec/doc/CDEM_product_specs.pdf)	25 m	GEM 2.5 and 1 km
	Shuttle Radar Topography Mission (SRTM) over USA (http://srtm.csi.cgiar.org/)	90 m	GEM 2.5 and 1 km
Soil texture	Global Soil Dataset for Use in Earth System Models (http://globalchange.bnu.edu.cn/research/soilw)	30 arc s	All
Land Cover	ESA CCI LC Global Map (European Space Agency Climate Change Initiative Land Cover; https://www.esa-landcover-cci.org/)	300 m	All

Hydrol. Earth Syst. Sci. Discuss., https://doi.org/10.5194/hess-2019-152
Manuscript under review for journal Hydrol. Earth Syst. Sci.
Discussion started: 23 April 2019

Table 3. Main characteristics of the different 6-h precipitation analysis used in this study. Details on the different precipitation backgrounds are given in Sect. 2.3.1 and Table 1. The different observation networks for precipitation are described in Sect. 2.1 and the location of the stations is shown on Fig. 1.

Name	Background	Observation network
CaPA 10 km Def	GEM 10 km	SYNOP
CaPA 10 km New	GEM 10 km	SYNOP, COOP, CRHO, ABE
CaPA 2.5 km	GEM 2.5 km	SYNOP, COOP, CRHO, ABE
CaPA 1 km	GEM 1 km	SYNOP, COOP, CRHO, ABE

5

Table 4. Main characteristics of hydrological simulations carried out with GEM-Hydro.

Experiment	Atmospheric forcing	Precipitation analysis	Initial surface conditions
10km_Def_OPL	GEM 10 km	CaPA 10 km Def	OPL
10km_Def_SND	GEM 10 km	CaPA 10 km Def	SND
10km_New_OPL	GEM 10 km	CaPA 10 km New	OPL
10km_New_SND	GEM 10 km	CaPA 10 km New	SND
2.5km_OPL	GEM 2.5 km	CaPA 2.5 km	OPL
2.5km_SND	GEM 2.5 km	CaPA 2.5 km	SND
1.0km_OPL	GEM 1.0 km	CaPA 1.0 km	OPL
1.0km_SND	GEM 1.0 km	CaPA 1.0 km	SND

10

Hydrol. Earth Syst. Sci. Discuss., https://doi.org/10.5194/hess-2019-152
Manuscript under review for journal Hydrol. Earth Syst. Sci.
Discussion started: 23 April 2019

Hydrology and Earth System Sciences
Discussions

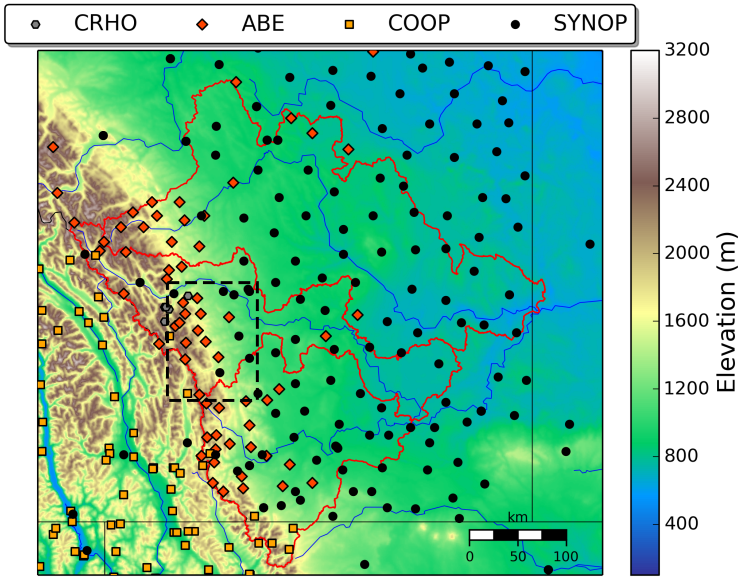

Figure 1: Map of southern Alberta showing the topography at 1-km resolution and locations of precipitation stations from different networks: USask's Canadian Rockies Hydrological Observatory (CHRO), Alberta Environment and Parks (ABE), the American meteorological cooperative network (COOP) and automatic synoptic stations (SYNOP) maintained by Environment and Climate Change Canada and other organizations. The red lines represent the Red Deer (north), Bow (middle) and Oldman (south) river basins. The dashed black box highlights the location of the Elbow and Highwood river basins.

Hydrol. Earth Syst. Sci. Discuss., https://doi.org/10.5194/hess-2019-152
Manuscript under review for journal Hydrol. Earth Syst. Sci.
Discussion started: 23 April 2019

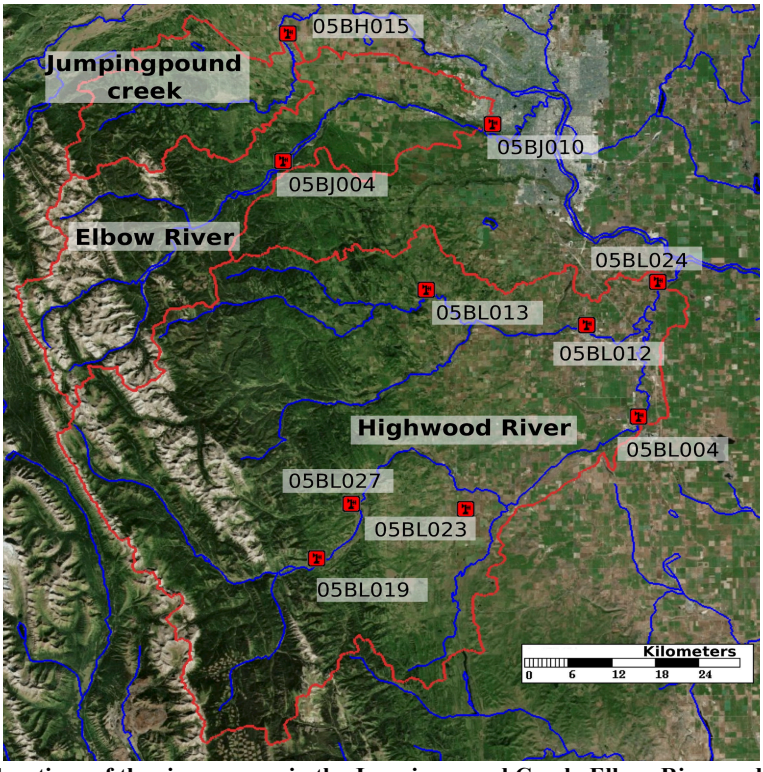

Figure 2: Map showing the locations of the river gauges in the Jumpingpound Creek, Elbow River and Highwood River basins used in this study. The general location of this area is shown on Fig. 1. The background map is taken from Microsoft VirtualEarth (2019).

Hydrol. Earth Syst. Sci. Discuss., https://doi.org/10.5194/hess-2019-152
Manuscript under review for journal Hydrol. Earth Syst. Sci.
Discussion started: 23 April 2019

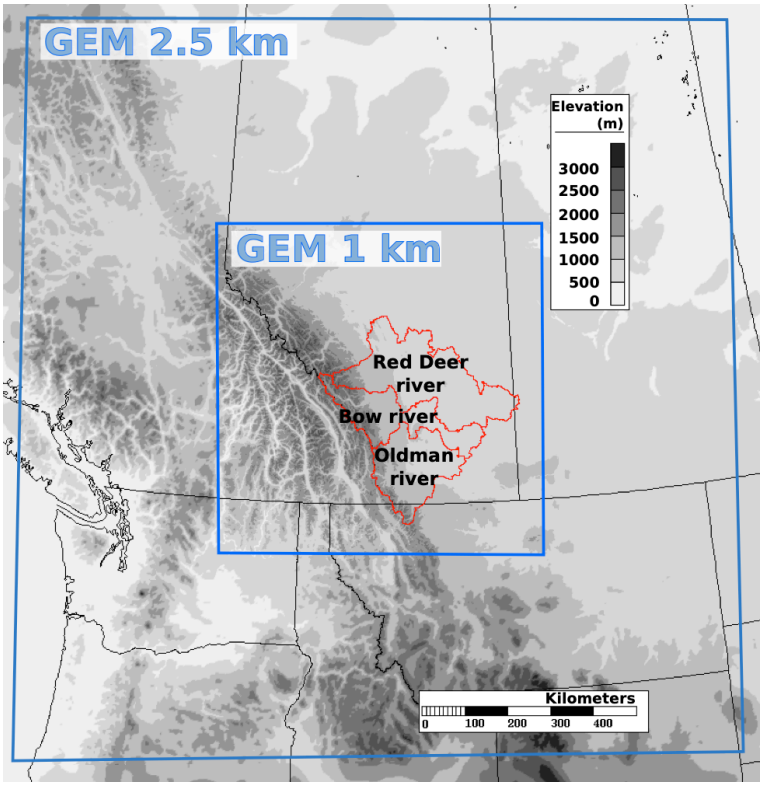

Figure 3. Location of the 2.5-km and 1-km GEM computational grids with elevation shown in shades of grey. The red lines represent the limits of the main river basins in southern Alberta.

Hydrol. Earth Syst. Sci. Discuss., https://doi.org/10.5194/hess-2019-152
Manuscript under review for journal Hydrol. Earth Syst. Sci.
Discussion started: 23 April 2019

Hydrology and Earth System Sciences
Discussions

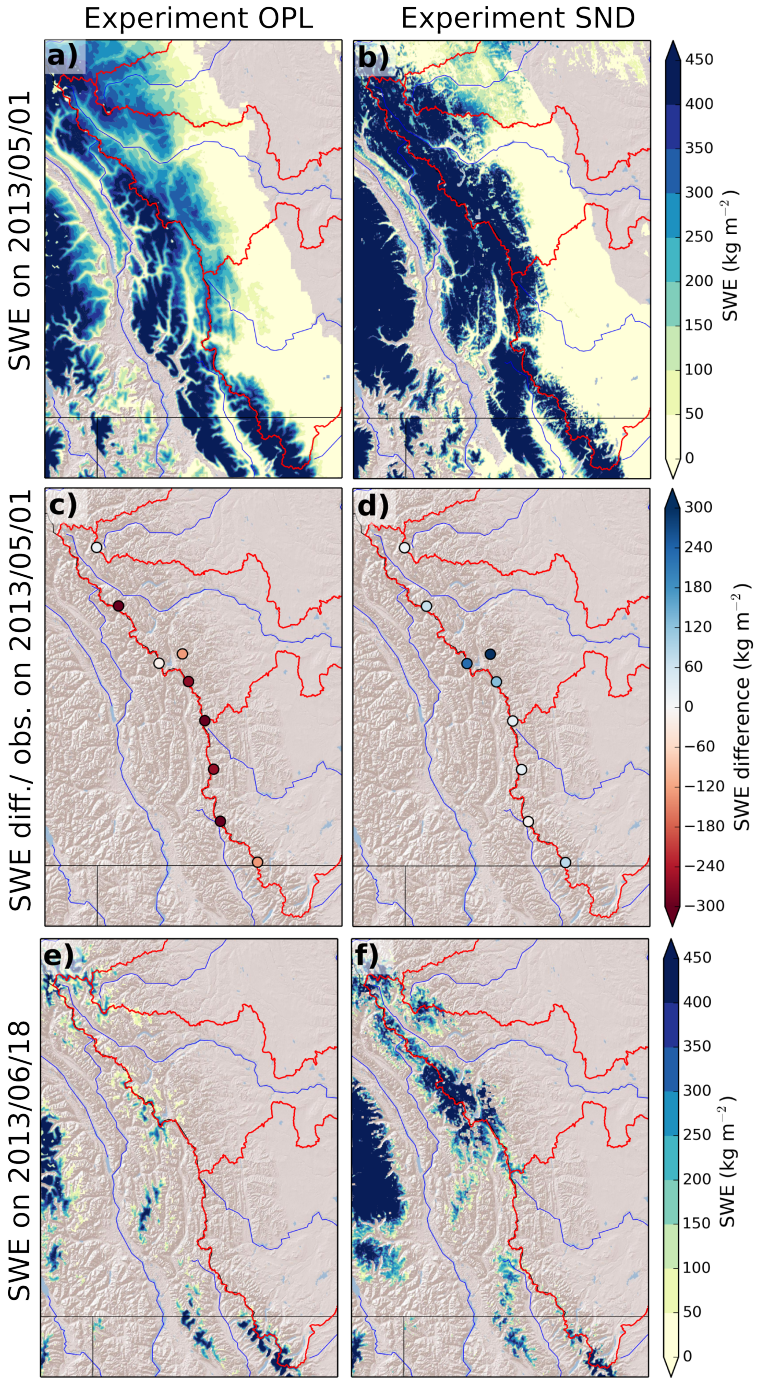

Figure 4. (Top) Snow water equivalent (SWE) on 1 May 2013 for two experiments: Open Loop (*OPL*) without insertion of SNODAS and (b) with insertion of SNODAS (*SND*). (Middle) SWE difference with observation from ABE snow pillows on 1 May 2013 for *OPL* (c) and *SND* (d). (Bottom) SWE on 18 June 2013 for *OPL* (e) and *SND* (f). The red lines on each figure represent the limits of the Bow, Oldman and Red Deer river basins (see Fig. 1 for general location).

Hydrol. Earth Syst. Sci. Discuss., https://doi.org/10.5194/hess-2019-152
Manuscript under review for journal Hydrol. Earth Syst. Sci.
Discussion started: 23 April 2019

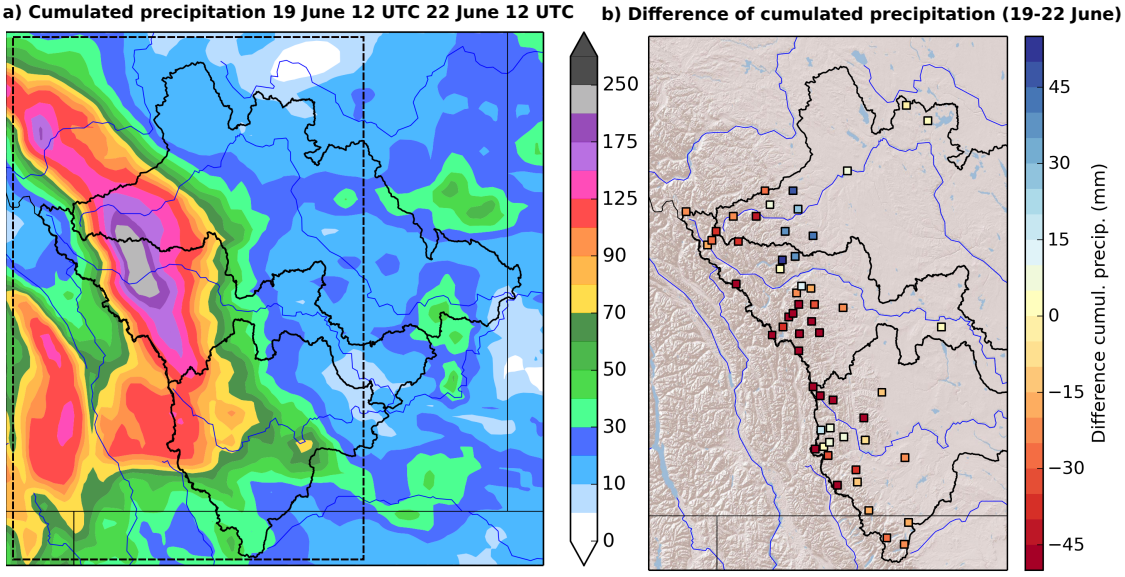

Figure 5 (a) Cumulated precipitation from 19 June 12 UTC to 22 June 12 UTC obtained with CaPA 10 km using only SYNOP stations. The 3-day total is obtained from the summation of successive 6-h precipitation analysis. The dashed line represents the limit of the area shown on (b). (b) Difference of accumulated precipitation between CaPA 10 km using default stations and measurements collected at CHRO, COOP and ABE stations that are not included in the analysis. The black lines on both figures represent the Bow, Oldman and Red Deer river basins (see Fig. 1 for general location).

Hydrol. Earth Syst. Sci. Discuss., https://doi.org/10.5194/hess-2019-152
Manuscript under review for journal Hydrol. Earth Syst. Sci.
Discussion started: 23 April 2019

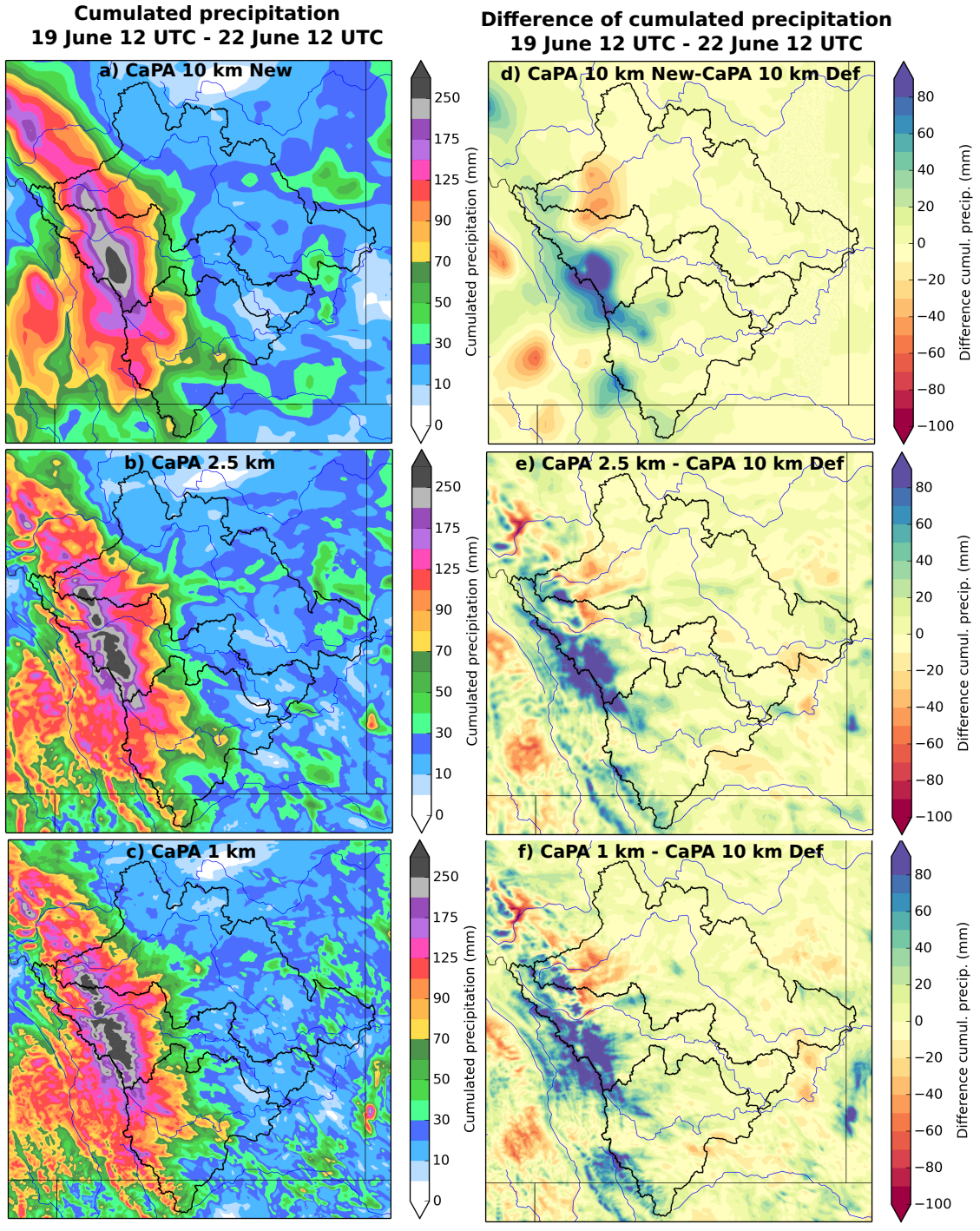

Figure 6. (Left) Accumulated precipitation from 19 June 12 UTC to 22 June 12 UTC obtained with CaPA using additional stations and precipitation background at (a) 10 km, (b) 2.5 km and (c) 1 km. (Right) Differences with the version of CaPA at 10 km using default stations. The black lines on each figure represent the Bow, Oldman and Red Deer river basins (see Fig. 1 for general location).

Hydrol. Earth Syst. Sci. Discuss., https://doi.org/10.5194/hess-2019-152
Manuscript under review for journal Hydrol. Earth Syst. Sci.
Discussion started: 23 April 2019

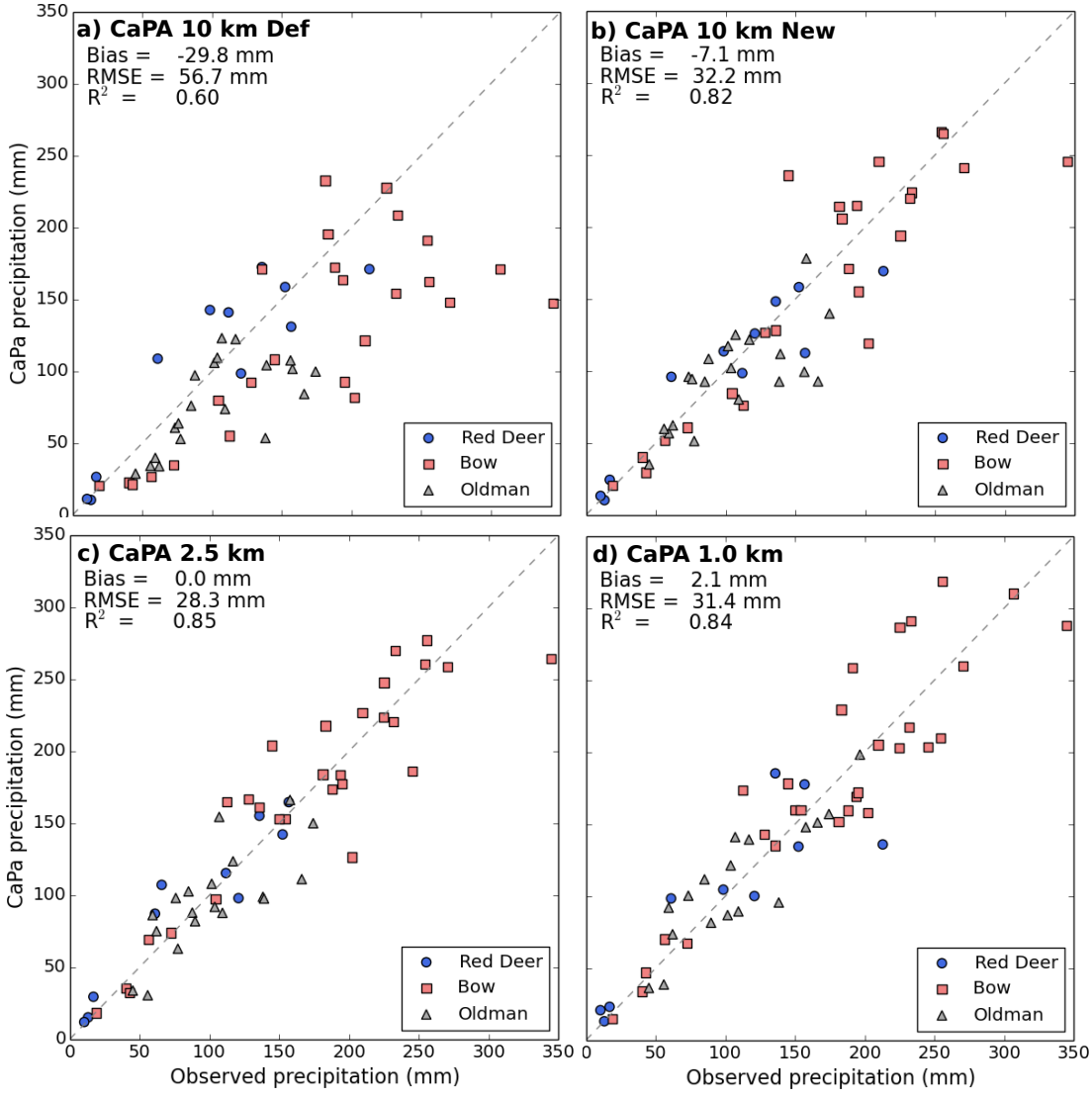

Figure 7. Scatter plot of accumulated observed precipitation at CHRO, COOP and ABE stations versus (a) precipitation from CaPA at 10 km using SYNOP stations (independent evaluation, same stations as Fig. 5b) and 6-h precipitation estimated by the leave-one out method for CaPA using all stations and precipitation background at (b) 10 km, (c) 2.5 km and (d) 1 km. Accumulated precipitation are computed from 19 June 12 UTC to 22 June 12 UTC. Error statistics (Bias, Root Mean Square Error (RMSE), and correlation coefficient, R^2) are given for each dataset.

Hydrol. Earth Syst. Sci. Discuss., https://doi.org/10.5194/hess-2019-152
Manuscript under review for journal Hydrol. Earth Syst. Sci.
Discussion started: 23 April 2019

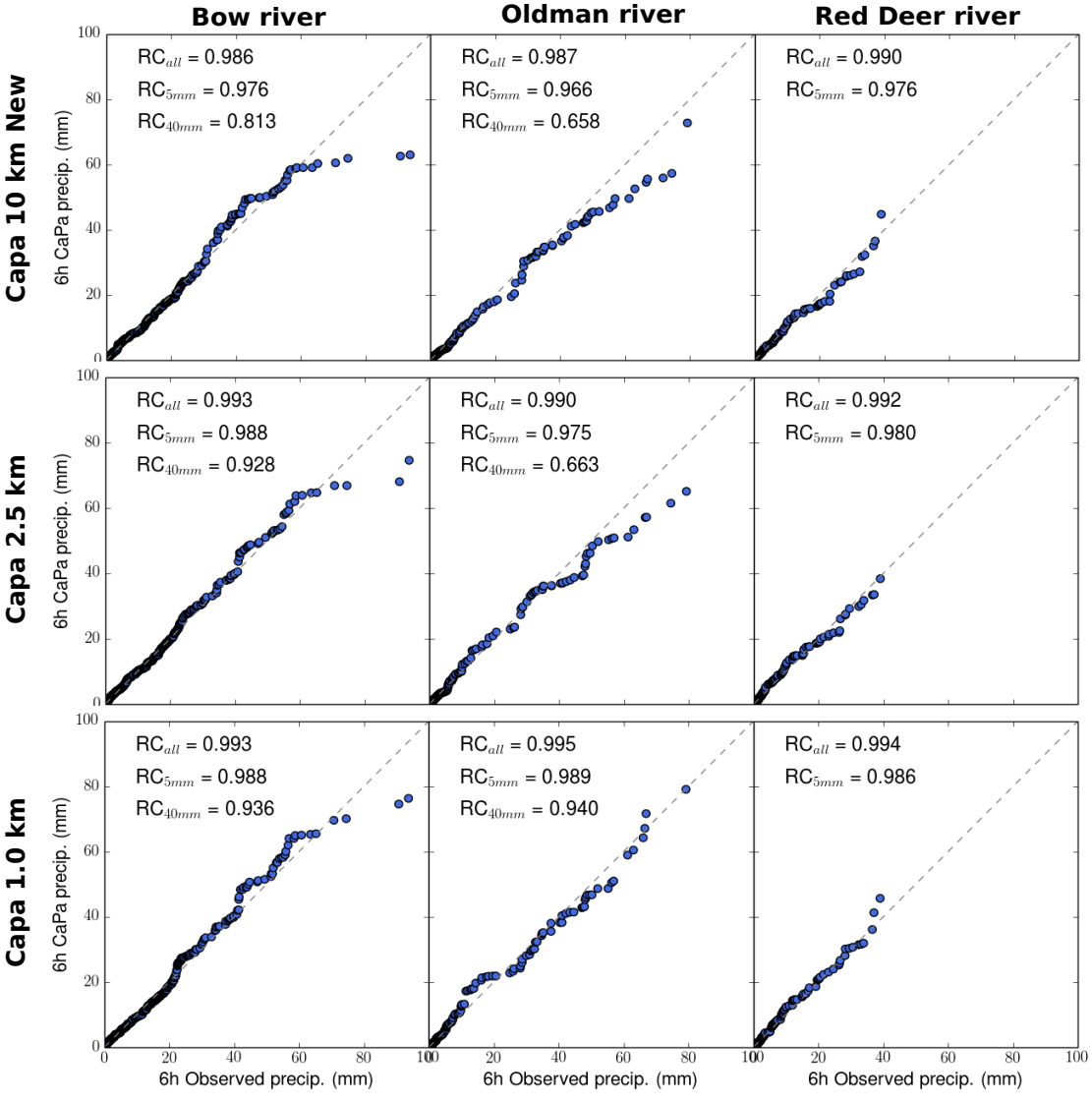

Figure 8. Quantile-quantile (QQ) plots between 6-h observed precipitation at CRHO, COOP and ABE stations and 6-h precipitation estimated by the leave-one out method for the different analysis: CaPA 10 km New (Top), CaPA 2.5 km (Middle) and CaPA 1 km (Bottom). The QQ plots are computed from 19 June 12 UTC to 22 June 12 UTC for the 3 main river basins in the region: Bow, Oldman and Red Deer. RC represents the concordance correlation coefficient (Lawrence and Lin, 1989) computed for different categories of 6-h precipitation: (i) all, (ii) above 5 mm and (iii) above 40 mm (see text for more details).

Hydrol. Earth Syst. Sci. Discuss., https://doi.org/10.5194/hess-2019-152
Manuscript under review for journal Hydrol. Earth Syst. Sci.
Discussion started: 23 April 2019

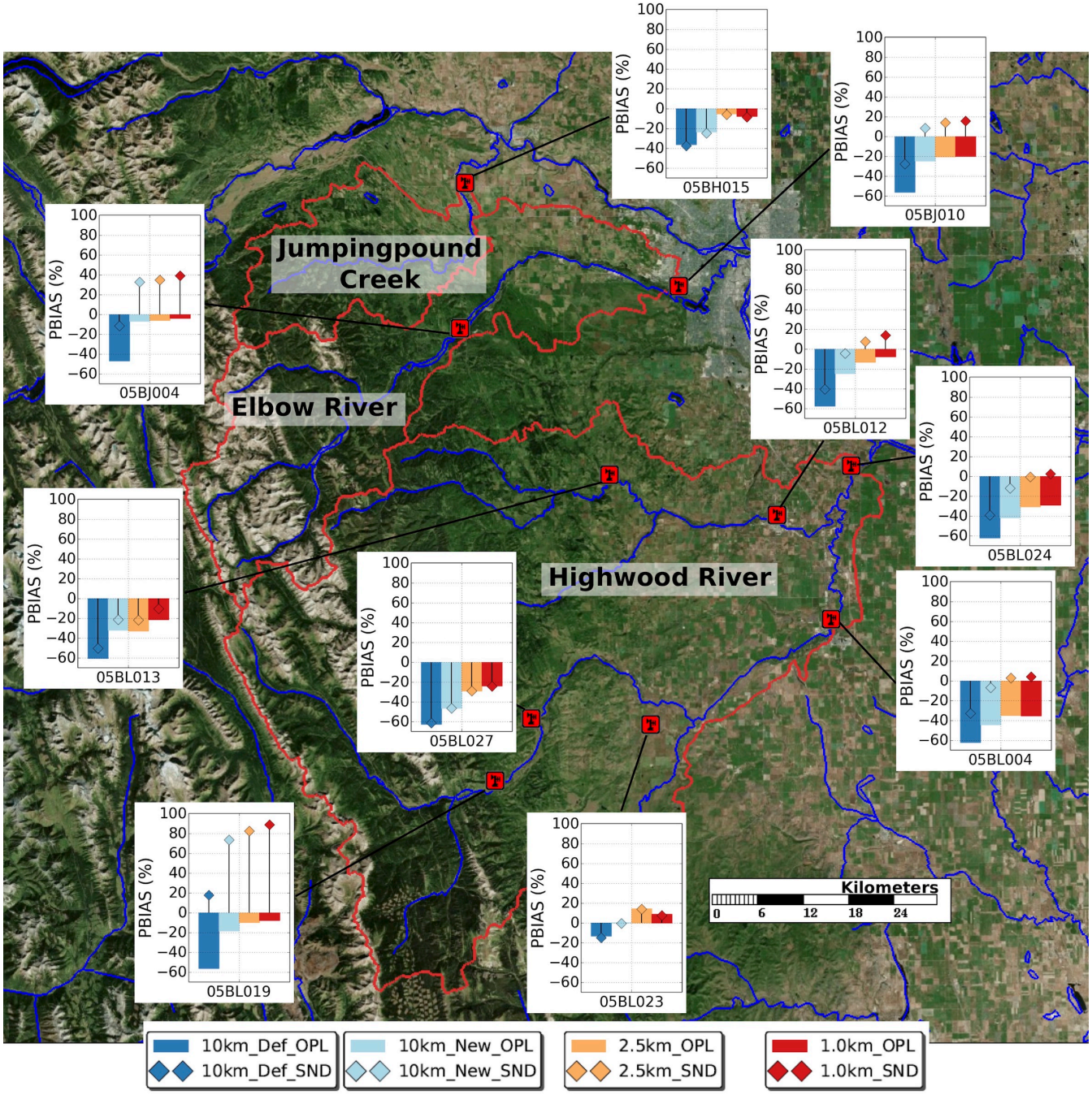

Figure 9. Map with inserted graphs for each hydrometric station showing the percent bias (PBIAS in %) in flood volume (from 20 0 UTC to 25 June 2013 0 UTC) for the different GEM-Hydro simulations. The diamonds indicates the results for the simulations using initial soil and snow conditions taken the *SND* experiment. The background map is taken from Microsoft VirtualEarth (2019).

Hydrol. Earth Syst. Sci. Discuss., https://doi.org/10.5194/hess-2019-152
Manuscript under review for journal Hydrol. Earth Syst. Sci.
Discussion started: 23 April 2019

Hydrology and Earth System Sciences
Discussions

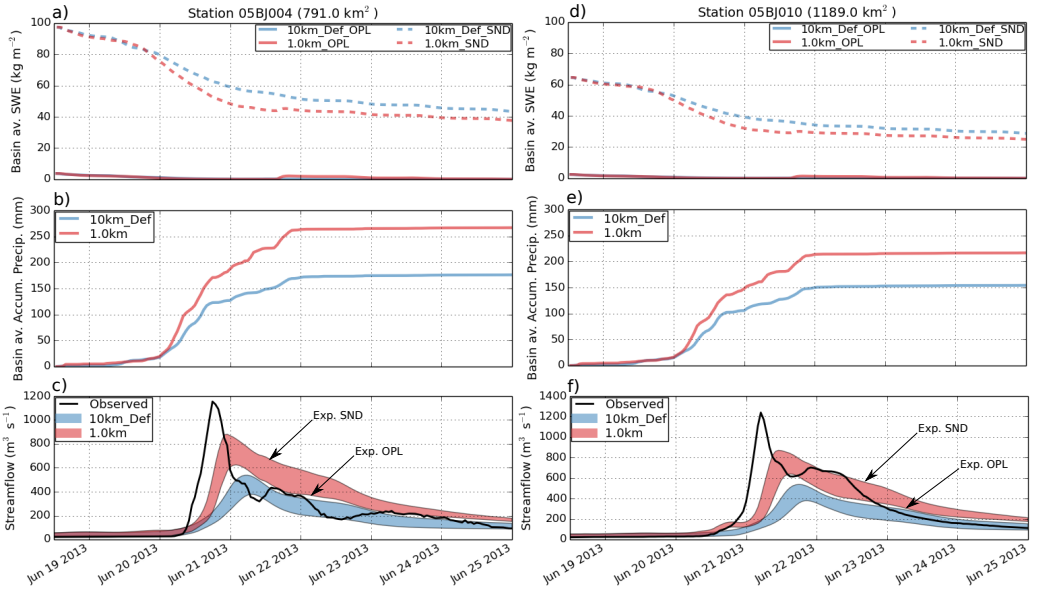

Figure 10. Results of hydrological simulations for 2 stations in the Elbow River Basin: station 05BJ004 (Left) and station 05BJ010 (Right). (a) & (d): Basin-averaged SWE for four GEM-Hydro simulations. (b) & (e): Basin-averaged accumulated precipitation for the corresponding atmospheric forcing. (c) & (f): Observed and simulated streamflow. For each filled area, the upper and lower limit represents the simulation using initial conditions from run *SND* and *OPL*, respectively. Note that the different *y* axis in (c) and (f).

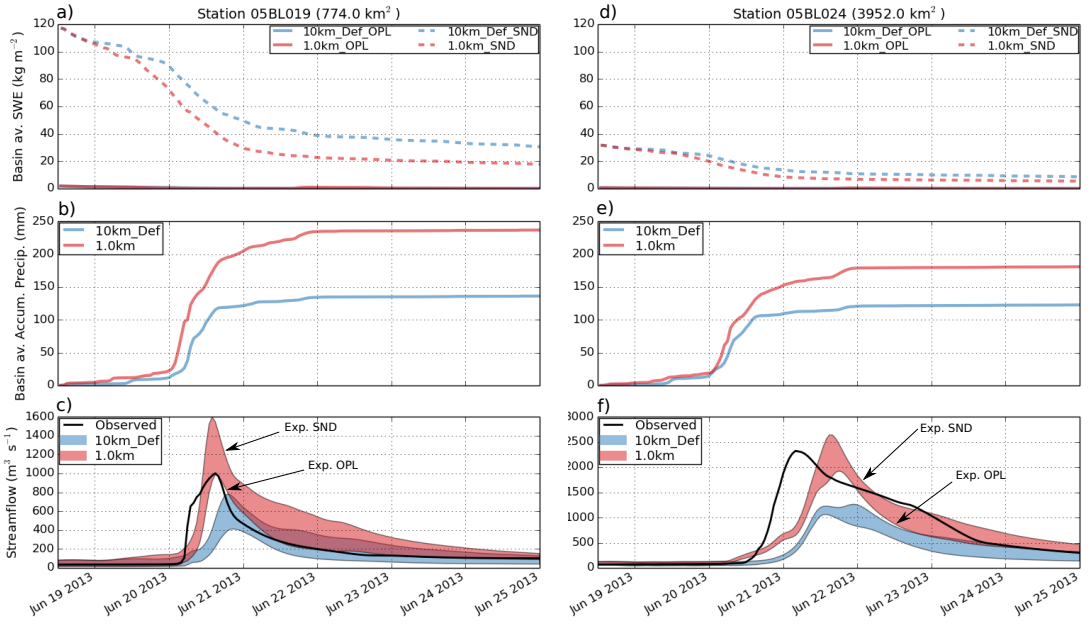

Figure 11. Same as Fig. 10 for 2 stations in the Highwood River Basin: station 05BL019 (Left) and station 05BL024 (Right). Note that the different *y* axis in (d) and (f).

Hydrol. Earth Syst. Sci. Discuss., https://doi.org/10.5194/hess-2019-152
Manuscript under review for journal Hydrol. Earth Syst. Sci.
Discussion started: 23 April 2019

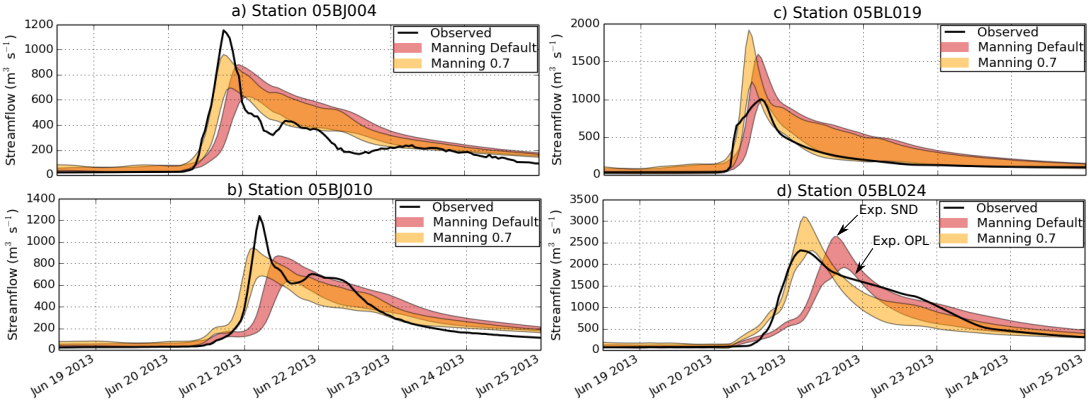

Figure 12. Observed and simulated streamflow at four stations in the Elbow River Basin (a & b) and the Highwood River Basin (c & d). Simulation results are taken from GEM-Hydro experiments using CaPA 1km and GEM 1km. For each filled area, the upper and lower limit represents the simulation using initial conditions from run *SND* and *OPL*, respectively. Two sets of Manning coefficient are tested for each experiment: default values (red area) and values reduced by 30 % (yellow area).